The spectral broadening of sound by turbulent shear layers. Part 2. The spectral broadening of sound and aircraft noise

By L. M. B. C. CAMPOS

Engineering Department, University of Cambridge†

It has been observed experimentally by Candel, Julienne & Julliand (1975) that a monochromatic test tone generated by a source inside a jet is received outside as a broad frequency band of definite shape. This phenomenon of spectral broadening occurs during transmission through the shear layer, which generally has a randomly irregular and unsteady shape, contains in addition distributed turbulence, and separates the jet and the ambient medium. We show in the first place that, in the audible range of frequencies, neither the approximation which treats the shear layer as a scattering interface with a convected undulating shape nor the opposite, high frequency limit obtained by means of asymptotic estimation of integrals derived for the diffraction of rays in turbulence is sufficient to provide a satisfactory theory of the observations. The refraction integrals obtained in part 1 have to be evaluated exactly in order to account for the phenomenon of spectral broadening, the methods used possibly being of interest in other branches of wave theory. The formation of the transmitted spectrum from an incident tone can be illustrated by representing a simple shear layer as an array of elements each re-radiating energy received from the source with its own characteristic attenuation and frequency shift. A computer program is used to obtain spectra under conditions corresponding to the experiments of Candel, Guédel & Julienne (1975) and gives encouraging agreement with their measurements, which were made with high frequency sources immersed in low speed jets. The theory can also be applied to the prediction of spectra received at various angles to the axis of high subsonic jets, but depends on extrapolation when supersonic exhausts are considered. We conclude with an example of the possible relevance of spectral broadening as a means of reducing the noise disturbance from current jet-powered aircraft, such as Concorde.

1. Introduction

The propagation of waves in a random medium, for example the transmission of sound through a turbulent shear layer, is accompanied by the transfer of energy into a wider band of frequencies. This phenomenon of spectral broadening is apparent when, say, a monochromatic source is located inside a jet and the field radiated to the ambient medium is received over a spectrum of definite shape. Understanding the connexion between the features of audible spectra and the physical properties of the

† Present address: R. Rodrigo da Funseca 91-2°D, Lisbon 1, Portugal.

shear layer could be a first step towards finding ways of modifying the latter in order to reduce the noise disturbance of current jet-powered aircraft.

1.1. *Aerodynamic refraction of jet noise*

The main practical stimulus for the study of aerodynamic acoustics has been the problem of jet noise, whose generation was originally modelled by Lighthill (1952) in a manner subsequently (1954) shown to be in basic agreement with experiment. The application of the theory to estimate the noise of aircraft (Lighthill 1962) is complicated by refraction in the shear layer between the turbulent jet and the ambient medium, which has been the subject of various attempts at theoretical modelling for more than a decade (e.g. Phillips 1960; Ffowcs Williams 1974). By using methods that may require further theoretical elucidation, Mani (1976; see also Balsa 1976a, b) has succeeded in obtaining directivities consistent with experiment at low frequencies. However the agreement deteriorates at high frequencies, for which refraction phenomena are more pronounced and where the noise disturbance of current jet aircraft appears to be more concentrated.

These refraction studies have been concerned with the directional distribution of energy, the spectra emitted by the sources being assumed to be unchanged during transmission except, possibly, for an overall frequency shift. However, Candel, Julienne & Julliand (1975) found that a test source emitting a monochromatic tone in the interior of a jet was received over a frequency range which is broader the higher the frequency of the original tone. The changes in the spectral shape under various conditions provide preliminary evidence that spectral broadening is associated with the presence of turbulence in the shear layer. The theoretical modelling should also take account of the irregular and unsteady interface that may be assumed to separate regions of the flow with different mean properties and thereby contribute to the random scattering of sound during transmission.

The theory of the scattering of sound by a static irregular interface (Howe 1976) has benefited from optical studies (Born & Wolf 1959), and the mathematical methods used in the present work to treat spectral as well as directional redistribution of energy (part 1) could also be applied to optics or other types of wave. This would be a continuation of the study of the scattering of electromagnetic waves by rough surfaces (Beckmann & Spizzichino 1963), which has already been applied to the sea clutter return of radar signals (Sholnik 1962) and to the reflexion of radio waves from the bed of glaciers and the surface of the moon (Berry 1973). In the case of acoustic waves there is the underlying question of the stability of shear layers, either free or excited by acoustic radiation (Jones 1974, 1977). Further references would only reinforce the impression that, whereas the aerodynamic generation of sound is well established with a fairly thorough theory, the refraction of jet noise is connected with matters requiring further study (e.g. the stability of shear layers, modifications of Kirchhoff's integration theory), and also basic observable phenomena such as spectral broadening appear to be largely unaccounted for.

1.2. *Acoustic and optical broadening*

Although we shall use the terminology of acoustics in treating the problem of sound propagation through a turbulent shear layer, our discussion may be extended without

much difficulty to the analogous problem in optics. For wavelengths much larger than the thickness of the shear layer the latter could be modelled as an undulating interface of steady shape which decomposes an incident monochromatic wave into a fundamental tone plus convection harmonics, as has been illustrated by considering a sinusoidal interface (Rayleigh 1945, vol. 2, p. 89) in motion (Clarke 1973). At high frequencies, for which the propagation through a thick layer of turbulence may be treated by means of the geometrical-acoustics approximation together with asymptotic estimation of diffraction integrals, the energy of an incident tone is spread over a continuous, smooth broad band, with the maximum at the source frequency. The former model of an interface with a steady shape is applicable at low frequencies, which do not appear to be dominant in jet noise, which is fortunate since sound of long wavelength is difficult to attenuate. On the other hand the asymptotic estimate of integrals derived using geometrical acoustics is valid only for frequencies near or beyond the limit of audibility.

A theory of the transmission of sound in the audible range of frequencies must therefore include the effects of an interface of random shape between the jet and the ambient medium as well as distributed turbulence in the shear layer. In addition the refraction integrals, which may also appear in other branches of wave theory, require exact evaluation, specifically by means of an expansion in power series followed by a multinomial expression in terms of Hermite polynomials leading to the ubiquitous Gaussian integrals. The low frequency limit corresponds to the zero-order term of the series, which appears as the incident tone (or spike) unchanged except for attenuation depending on the ratios of certain scales of the shear layer to the wavelength of sound, i.e. greater the higher the tone frequency. The subsequent terms of the series form side bands which generally exhibit a dip near the spike, rise smoothly over frequencies *not* found in the source, and finally decay in a manner which is reminiscent of the asymptotic case and corresponds to the higher-order terms of the series.

A side band can be constructed from a model array of re-radiating elements each of which transmits the incident energy (from the source) with its own attenuation and frequency shift and is therefore responsible for one interval of the spectrum received by the observer. The formulae evincing these general properties can also be used in a computer program to predict the spectra transmitted through a shear layer from a source in the interior of a jet to an observer in the ambient medium. Comparison of computed spectra under conditions corresponding to the experiments of Candel, Guédel & Julienne (1975) shows encouraging agreement (figures 3 and 4) for different shear-layer scales, low jet speeds and high source frequencies. The spectra received in directions away from the vertical can be predicted for low speed as well as for high subsonic jets (figure 2), though in the latter case accurate measurements with test sources might be difficult to perform.

1.3. *Attenuation of audible disturbances*

Some work whose value stands comparison with the voluminous recent literature was published by Rayleigh, curiously enough *not* in his authoritative treatise on acoustics (first published in 1877, see Rayleigh 1945), but in a series of three papers published over a period of four decades (1873, 1889, 1915). These were concerned with the optical phenomenon of 'widening of spectrum lines' of a substance (under chemical

analysis), which he ascribed to scattering by gas molecules with a velocity distribution satisfying a Maxwellian law. The phenomenon underlying the spectral broadening of sound diffracted by turbulence is not very different, the random velocity fluctuations of turbulence causing phase shifts described by a Gaussian probability distribution (see part 1, Campos 1978). The lucidity and conciseness of Rayleigh's exposition (e.g. 1915) are as exemplary as ever, and 'were he alive today ... he might be taking an interest' (Lighthill 1962) in the problem of aircraft noise, which undoubtedly he would have solved.

The present theory applies to the transmission of sound through a shear layer of moderate supersonic speed as far as the effects of distributed turbulence and changes in density (and sound speed) are concerned. The effect of shock waves on the refraction of sound is represented by a modification of the scattering and diffraction scales, in order to perform a preliminary assessment of spectral broadening in the important practical case of Concorde. It is shown in figure 5 that if the thickness and degree of irregularity of the shear layer are doubled then a discrete tone emitted by a flow source within the exhaust at a frequency of 8 kHz (corresponding to the order of magnitude of the turbine rotation speeds of modern turbojet engines) will be transmitted as broad-band noise, which is audibly less objectionable (about 10 dB below). How to make the shear layer twice as thick and irregular without reinforcing the sources, which could detract from the attenuation envisaged, is a matter of conjecture that only experiment is likely to settle.

Our account of spectral broadening proceeds from the theoretical to the practical point of view through the following stages: in §2 the results of part 1 are taken as the starting formulae for an analysis of spectra, in the first instance in the low and high frequency limits to evince some of the features subsequently found combined in the intermediate audible range; in §3 the phenomenon of spectral broadening is reviewed as a formal evaluation of refraction integrals, and is illustrated by the model of an array of re-radiating elements; in §4 computed and measured spectra are compared for low jet speeds, for which experiments with test sources are available, high subsonic directional spectra are predicted and the extension to supersonic exhausts gives some hope regarding the possibility of reducing jet noise. The exposition includes a number of illustrations (figures 1–5) which could be of some interest to readers concerned with jet noise as a brief recollection of some of the features of spectral broadening of sound.

2. The analysis of frequency spectra

In order to ascertain which model of a shear layer might be applicable to audible disturbances we shall take $l = 10$ cm as a typical scale of flow in the shear layer. The model of an interface of steady shape applies only to wavelengths $\lambda \gg l$, e.g. $\lambda \gtrsim 100$ cm, corresponding to frequencies $\omega \lesssim 300$ Hz, which are only slightly attenuated by small-scale distributed inhomogeneities of the medium. The geometrical-acoustics theory of diffraction at high frequency by shear-layer turbulence requires that $\lambda M' \ll l$ and the asymptotic estimation of integrals imposes the more restrictive condition $\lambda^2 \ll M'^2 l^2$, where the perturbation Mach number M' is low even for moderately supersonic jets, and in these cases the upper limit of audibility $\lambda \simeq 1\cdot7$ cm (in air at one atmosphere) is exceeded, i.e. the model would then apply mostly to ultrasonic

sound. Neither approximation seems adequate over the full audible range 20 Hz–20 kHz nor, in particular, in the higher range of frequencies where refraction effects are more marked and the noise disturbance from aircraft is concentrated. A study of low and high frequency limits does, however, serve to introduce some of the distinctive features of spectra which are observed combined in a modified form in the audible range.

2.1. *Discrete tones at low frequency*

We consider (figure 1*b*) a point source of frequency ω_0 convecting at constant velocity **U** within a jet of velocity **V**, density ρ and sound speed c. This jet is separated from a stationary ambient medium of mean density ρ_0 and sound speed c_0 by a shear layer, in which the mean velocity is α**V** $(0 < \alpha < 1)$. The wave field radiated into the ambient medium is described by the spectral directivity $I(\theta, \phi, \omega)$, which specifies the energy flux at frequency ω per unit solid angle at a location defined by the spherical polar co-ordinates (θ, ϕ) of the observer relative to the source at the time of emission of the sound:

$$I(\theta, \phi, \omega) = (64\pi^5 \rho_0 c_0^3)^{-1} \{\sin^2 \theta \cos^2 \phi / (1 - M_0 \cos \theta)\} \int^{\mathrm{Re}\,(\gamma, \Gamma)} |\omega S / A\gamma|^2$$

$$\times \exp\{i(\mathfrak{g} - \mathbf{G}) . \mathbf{z} + i\{\omega - \omega_0 - \mathfrak{g} . \mathbf{U} + \alpha\mathbf{V} . (\mathfrak{g} - \mathbf{G})\} t\} C(\mathbf{z}, t) d^2g \, d^2z \, dt. \quad (1)$$

This formula is derived in part 1 [formula (63*a*), with substitutions from (62*a–c*)]; $\mathfrak{g} \equiv (g_1, g_2)$ is the horizontal wave vector (in the shear-layer mean plane) of the sound emitted by the source and **G** the horizontal wave vector received by the observer, i.e. $\mathbf{G} = (\omega/c_0)(\cos \theta, \sin \theta \sin \phi)$. It is assumed that $\mathfrak{g}$ is conserved across the shear layer and is related to γ and Γ, the incident and transmitted normal wavenumbers (or x_3 components of the wave vectors), which are given by

$$\Gamma(\mathfrak{g}) = \{(\omega_0 + \mathfrak{g} . \mathbf{U})^2 / c_0^2 - g^2\}^{\frac{1}{2}}, \qquad \gamma(\mathfrak{g}) = \{[\omega_0 + \mathfrak{g} . (\mathbf{U} - \mathbf{V})]^2 / c^2 - g^2\}^{\frac{1}{2}}, \quad (2a, b)$$
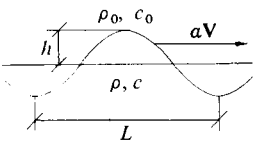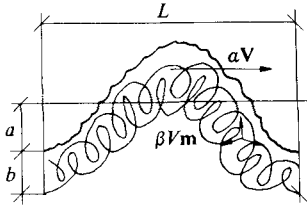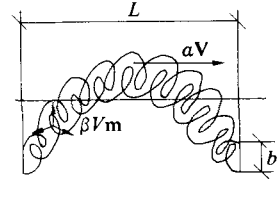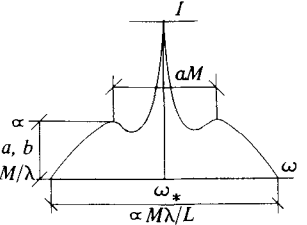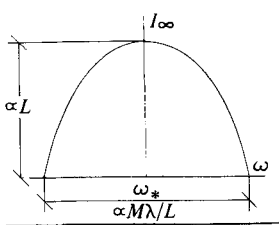
$$S(\mathfrak{g}) = S(i\mathfrak{g}, i\gamma, -i\omega_0 - i\mathfrak{g} . \mathbf{U}), \quad A(\mathfrak{g}) = 1 + (\rho/\rho_0)(1 - M \cos \theta) \Gamma/\gamma. \quad (2c, d)$$

The function S indicates the multipolar character of the source, having originally appeared as an operator $S(\nabla, \partial/\partial t)$ applied to the forcing term of the wave equation [part 1, formula (22)]; the amplitude factor in the transmission coefficient for an incident plane wave is $2/A$ [part 1, formula (4*b*)] and we have denoted by

$$(M, M_0) \equiv (V, U)/c_0$$

the Mach numbers of the source and jet.

The general expression (1) for the spectral directivity involves integrations with respect to **z** and t over the mean plane of the shear layer and all time, and depends on a characteristic function $C(\mathbf{z}, t)$ containing the phase shifts associated with transmission through the layer. For example, the phase shift for scattering by an irregular interface is given by $(\gamma - \Gamma)\xi$ [part 1, equation (4*a*)], where ξ is the displacement of the interface from the mean plane $x_3 = 0$, e.g. $\xi = h(z)$ for a shape consisting of corrugations perpendicular to the mean-flow direction $(z \equiv z_1)$. If the wavelength of the sound is much larger than the thickness of the shear layer the latter behaves like a sharp interface of steady undulating shape. The scale of the undulations will depend on the typical size L of the eddies in the jet flow, convected at, say, a velocity α**V** (where $0 < \alpha < 1$) and corresponding to a Strouhal frequency $\omega_e \simeq L/\alpha V$. As an example of the transmission of sound at very low frequencies we consider a convected

$\lambda \gg b$	$a^2 \ll L^2 \cong \lambda^2 \ll b^2$ $a^2 \cong \lambda^2 \ll L^2,\ b^2$	$\lambda \ll b^2/M'^2$
Infrasound	Audible range	Ultrasound

Source tone and symmetric series of convection harmonics	Spike + side bands Spike: attenuated source tone Side bands: an interference effect	Continuous, smooth, convex broad band with maximum at source frequency

(a)
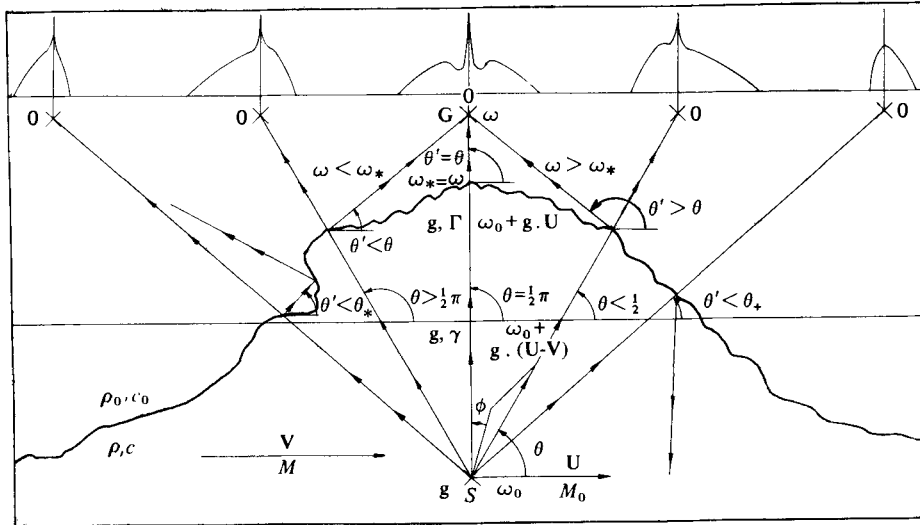
(b)

FIGURE 1. General theoretical properties. (a) Shape and parameters of spectra. (b) Model and properties of refraction.

periodic interface, of height h and nodal distance L, whose characteristic function $C_-(z) \equiv \exp\{i(\gamma - \Gamma)h(z/L)\}$ is given by the following Fourier series expansion:

$$C_-(z) = \sum_{n=-\infty}^{+\infty} D_n(\gamma - \Gamma)\exp\{inz/L\}, \tag{3a}$$

$$D_n(\gamma - \Gamma) \equiv \frac{1}{2\pi} \int_0^{2\pi} \exp\{i\{(\gamma - \Gamma)h(y) - ny\}\}\, dy. \tag{3b}$$

In the classical case of a sinusoidal interface $h(y) = h \sin y$, the real part of the Fourier coefficient D_n would be a Bessel function $\hat{J}_n(h\{\gamma - \Gamma\})$ of the first kind and order n (Watson 1927). On substitution of each term of (3a) into (1), the space–time integrations give $(2\pi)^3$ times the product of delta functions

$$\delta(g_1 - G_1 + n/L)\,\delta(g_2 - G_2)\,\delta(\omega - \omega_0 - g_1\,U + \alpha V(g_1 - G_1)),$$

which permits the d^2g integral to be performed trivially, after which the remaining delta function implies that the spectrum consists of discrete tones.

The frequency of the nth tone ($n = -\infty, ..., +\infty$) is given by

$$\omega_n = \omega_* + n(\alpha V - U)/L, \quad \omega_* = \omega_0/(1 - M_0 \cos\theta) \qquad (4a, b)$$

(where $M_0 = U/c_0$) and differs from the frequency ω_0 of the source Doppler shifted to ω_*, when in motion, by a multiple of $\Delta\omega \equiv (\alpha V - U)/L$. The latter is associated with the convection of interfacial undulations of scale L at a velocity $\alpha V - U$ relative to the source. To each tone, or convection harmonic, there corresponds an energy lobe, given by $(2\pi)^3$ times the integrand of (1):

$$J_n(\theta, \phi) = \frac{(\rho_0 c_0)^{-1}}{8\pi^2} \frac{\sin^2\theta \sin^2\phi}{1 - M_0 \cos\theta} \left\{\frac{\omega_n}{c_0}\right\}^2 \left[\frac{SS^*}{A^2\gamma^2}\right], \qquad (5)$$

where the asterisk denotes the complex conjugate and the expression in square brackets is calculated for $G_1 = g_1 + n/L$, $G_2 = g_2$ and $\omega = \omega_n$. The complete solution specifying the low frequency spectral directivity is therefore

$$I_-(\theta, \phi, \omega) = J_0(\theta, \phi)\,\delta(\omega - \omega_*) + \sum_{\substack{n = -\infty \\ n \neq 0}}^{+\infty} J_n(\theta, \phi)\,D_n(\gamma - \Gamma)\,\delta(\omega - \omega_n) \qquad (6)$$

and consists of the directivity J_0 of a plane interface at the fundamental Doppler-shifted source frequency ω_n plus a symmetric series of tones (and the corresponding lobes), i.e. convection harmonics of frequency ω_n and directivity J_n (see infrasound in figure 1a). For the case (Clarke 1973) of a sinusoidal interface $h(y) = h \sin y$ and

$$D_n = O(|h(\gamma - \Gamma)|^n) \simeq O(\{h/\lambda\}^n),$$

so that higher-order convection harmonics have a decreasing amplitude for $h/\lambda < 1$. The latter result was first obtained by Rayleigh (1945, vol. 2, pp. 89–96) for a static sinusoidal interface, for which case all the lobes (5) are evaluated at the fundamental frequency (4b). The sequence of convection harmonics also disappears for a plane interface (even in motion), giving

$$I_0(\theta, \phi, \omega) = \lim_{h/\lambda \to 0} I_-(\theta, \phi, \omega) = J_0(\theta, \phi)\,\delta(\omega - \omega_*), \qquad (7)$$

in which the plane-layer directivity, given by (5) with $\mathbf{G} = \mathbf{g}$ and $\omega = \omega_*$, is consistent with Howe (1975).

2.2. *Continuous broad band at high frequencies*

At the opposite extreme of high frequencies the shear-layer model must take account of the diffraction of sound rays by the turbulence within the shear layer. It can be predicted theoretically and appears to be consistent with experimental evidence that (part 1, § 4.1) the statistics of the phase shift of waves transmitted through the shear

layer are Gaussian and can be specified by means of the high frequency characteristic function
$$C_+(z_i) = \exp\{-\beta^2 M^2 (c_0/c)^2 k^2 b^2 \csc \theta[1 - E(z_i)]\}, \tag{8}$$

in which $z_i \equiv (t, \mathbf{z})$ where $i = 0, 1, 2$ are the co-ordinates of scattering events consisting of a time delay and spatial separation. For uncorrelated events $E \simeq 0$ and (8) reduces to an attenuation $\exp(-Q_+)$, where Q_+ is equal to the product of the squares of the Mach number of the turbulence $\beta M(c_0/c)$, the wavenumber $k \equiv \{g^2 + \gamma^2\}^{\frac{1}{2}}$ and the thickness b of the layer and is increased by a factor of $\csc \theta$ for oblique incidence. In general (8) involves the autocorrelation coefficient

$$E(z_i) = \prod_{i=0}^{2} (1 - 2z_i^2/L_i^2) \exp\{-(z_i/L_i)^2\}, \tag{9}$$

where (part 1, §4.2) L_0 is the refraction time and L_1 and L_2 are the longitudinal and transverse refraction lengths (i.e. in the direction x_1 of the mean shear flow and in the perpendicular direction x_2 parallel to the shear-layer mean plane $x_3 = 0$). Scattering events separated by less than a correlation scale ($z_i < L_i$, $i = 0, 1, 2$) interfere, resulting in the amplification factor $\exp(Q_+ E)$ in (8), but since $E < 1$ for separate events, this compensates only partially for the independent attenuation $\exp(-Q_+)$.

If the thickness of the shear layer is very large compared with the wavelength of the sound divided by the Mach number of the turbulence, so that $Q_+ \gg 1$, the asymptotic approximation to (8) is obtained by expanding (9) in powers of $(z_i/L_i)^2$ to first order, to give the asymptotic characteristic function:

$$C_\infty(z_i) = \exp\{-[(z_1/\mathscr{L}_1)^2 + (z_2/\mathscr{L}_2)^2 + (z_0/\mathscr{L}_0)^2]\}, \tag{10a}$$

$$\mathscr{L}_i^{-2} \equiv (3/L_i^2)\beta^2 M^2(c_0/c)^2 k^2 b^2 \csc \theta. \tag{10b}$$

The characteristic function $C_+ = \exp\{-Q_+(1-E)\} = (1-Q_+) + Q_+ E + O(Q_+^2)$ depends linearly on the autocorrelation coefficient E to the first order in Q_+, i.e. for small attenuation $Q_+^2 \ll 1$. In the opposite asymptotic limit of large attenuation ($Q_+ \gg 1$) (10a) resembles the 'autocorrelation functions' which are sometimes introduced empirically (e.g. Chernov 1967, chap. 1). However, even in this limiting case the autocorrelation and characteristic functions have distinct properties, e.g. the asymptotic refraction scales defined by (10b) depend not only on the properties of the wave-bearing medium but also on the wavelength of sound: $\mathscr{L} \propto \lambda$. When (10a) is used to give an asymptotic estimate of (1), the latter reduces to the product of three Gaussian integrals and leads to an expression which (as will be proved in §3.1) is valid to $O(\mathscr{L}_i^4)$:

$$I_\infty(\theta, \phi, \omega) = \Theta(\theta, \phi) \int^{\mathrm{Re}(\gamma, \Gamma)} \Lambda_\infty(\mathbf{g}, \omega, \mathbf{G}) \exp\{-\Omega_\infty(\mathbf{g}, \omega, \mathbf{G})\} d^2 g, \tag{11}$$

where we have distinguished the observation, amplitude and broadening functions Θ, Λ_∞ and Ω_∞, respectively. The asymptotic spectral directivity I_∞ is determined by evaluating the integral (11) for propagating incident and transmitted wave modes at the shear layer, corresponding to real values of γ and Γ only. In each observation direction (θ, ϕ), the conditions $\mathrm{Re}(\gamma, \Gamma)$ define a range of frequencies (ω_1, ω_2) or

$$\omega_1 < \omega < \omega_2$$

over which a continuous broad band of sound can be received.

Appearing first in the asymptotic spectral directivity (11) is the observation function

$$\Theta(\theta, \phi) \equiv (64\pi^{\frac{1}{2}}\rho_0 c_0)^{-1} \sin^2\theta \sin^2\phi (1 - M_0 \cos\theta)^{-1}, \tag{12}$$

which must be multiplied by $2\pi^{\frac{1}{2}}$ whenever one of the refraction scales is infinite [see (28)], e.g., for a plane interface devoid of turbulence, the multiplying factor is $(2\pi^{\frac{1}{2}})^3$, giving a net numerical coefficient of $1/8\pi^2$ in agreement with (5). Next, the asymptotic amplitude function is defined by

$$\Lambda_\infty(\mathbf{g}, \omega, \mathbf{G}) \equiv (|S|K/\gamma)^2 \prod_{i=0}^{2} \{\mathscr{L}_i + O(\mathscr{L}_i^4)\}, \tag{13a}$$

$$K \equiv \omega/c_0, \quad k \equiv \{g^2 + \gamma^2\}^{\frac{1}{2}} = \{\omega_0 + \mathbf{g}.(\mathbf{U} - \mathbf{V})\}/c_0. \tag{13b,c}$$

The wavenumber (13b) received in the ambient medium, which is different from the wavenumber (13c) emitted in the jet, appears in Λ_∞, which is proportional to the square of the modulus of the strength S of the source divided by γ and (to the fifth order of approximation) to the product of the asymptotic refraction scales $\mathscr{L}_0 \mathscr{L}_1 \mathscr{L}_2$. The latter also appear in

$$4\Omega_\infty(\mathbf{g}, \omega, \mathbf{G}) = (g_1 - G_1)^2 \mathscr{L}_1^2 + (g_2 - G_2)^2 \mathscr{L}_2^2 + \{\omega - \omega_0 + \mathbf{g}.\mathbf{U} + \alpha\mathbf{V}.(\mathbf{g} - \mathbf{G})\}^2 \mathscr{L}_0^2, \tag{14}$$

which is asymptotically independent of the frequency since $\mathscr{L} \propto \omega^{-1}$. The spectral-broadening function Ω_∞ occurs in the exponential in (11), and shows that the spectrum is a smooth, convex broad band decreasing monotonically on either side of the maximum, which occurs for direct transmission from the source at $\mathbf{g} = \mathbf{G}$, $\omega = \omega_*$ (see ultrasound in figure 1a).

2.3. *Spike and side bands in the audible range*

For the reasons stated earlier (at the beginning of §2), in order to model the strong refraction in the upper audible range we must consider both the scattering by an irregular interface of random unsteady shape and the diffraction by the turbulence and evaluate the spectral directivity integrals without making asymptotic or other approximations. There are in general two contributions to the attenuation factor Q:

$$Q = a^2(\gamma - \Gamma)^2 + \beta^2 M^2(c_0/c)^2 k^2 b^2 \operatorname{cosec}\theta, \tag{15}$$

in which the second term, which appears in (8), is associated with diffraction by turbulence and the first term with scattering by interfacial irregularities of r.m.s. height a. The general characteristic function for a shear layer is $C = \exp\{-Q(1 - E)\}$, and may be expanded exactly in a power series in the autocorrelation coefficient (9), giving

$$C(z_i) = \exp(-Q) \sum_{n=0}^{\infty} (Q^n/n!) \prod_{i=0}^{2} (1 - 2z_i^2/L_i^2)^n \exp\{-n(z_i/L_i)^2\}. \tag{16}$$

The symmetry of the space–time dependence $z_i \equiv (t, \mathbf{z})$ in (16) shows that the spectral directivity can be expressed in the (exact) form

$$I(\theta, \phi, \omega) = \Theta(\theta, \phi) \sum_{n=0}^{\infty} \frac{1}{n!} \int^{\operatorname{Re}(\gamma, \Gamma)} \{\omega|S|/A\gamma\}^2 \exp(-Q) Q^n$$
$$\times I_n(g_1 - G_1; L_1) I_n(g_2 - G_2; L_2) I_n(\omega - \omega_0 - g_1 U + \alpha V(g_1 - G_1); L_0) d^2g, \tag{17}$$

in which I_n is an interference integral defined by

$$I_n(g-G;L) \equiv \pi^{-\frac{1}{2}} \int_{-\infty}^{+\infty} (1 - 2z^2/L^2)^n \exp\{i(g-G)z - nz^2/L^2\} dz$$

$$= \frac{L}{n^{\frac{1}{2}}} \exp\left\{ -\frac{(g-G)^2 L^2}{4n} \right\} \sum_{r=0}^{n} \frac{(2n)^{-r} n!}{(n-r)!\, r!} H_{2r}\left\{ \frac{(g-G)L}{2n^{\frac{1}{2}}} \right\}, \qquad (18)$$

where $H_{2r}(v) \equiv \exp(v^2)(d^{2r}/dv^{2r})\exp(-v^2)$ are the Hermite polynomials of order $2r$. We note that each factor z in the non-exponential part of the integrand in (18) corresponds to a differentiation $\partial/\partial\{i(g-G)\}$, so that the integral may be evaluated by applying $\{1 + 2\partial^2/\partial\{(g-G)L\}^2\}^n$ to a standard Gaussian-type integral. The latter is equal to $L/n^{\frac{1}{2}}\exp(-v^2)$, where $v \equiv (g-G)L/2n^{\frac{1}{2}}$, i.e. the first factor on the right of (18), which should be multiplied by a polynomial of order $2n$ in v, viz.

$$p_{2n}(v) \equiv \exp(v^2)\{1 + (2n)^{-1}d^2/dv^2\}^n \exp(-v^2).$$

Formal use of the binomial theorem enables the result to be expressed in terms of Hermite polynomials $H_{2r}(v) \equiv \exp(v^2)(d^{2r}/dv^{2r})\exp(-v^2)$ with $r = 1, \ldots, n$ (Courant & Hilbert 1966, vol. 1, p. 91), giving the expression on the right of (18).

The zero-order term in the expansion (16) reduces to $\exp(-Q)$, and for this case (1) may be evaluated trivially in terms of delta functions, giving the first contribution to the audible spectral directivity, whose complete form is

$$I(\theta, \phi, \omega) = J_0(\theta, \phi)\exp(-Q)\,\delta(\omega - \omega_*)$$

$$+ \Theta(\theta, \phi)\sum_{n=1}^{\infty} \int^{\mathrm{Re}(\gamma,\Gamma)} \Lambda_n(\mathbf{g}, \omega, \mathbf{G})\exp\{-\Omega_n(\mathbf{g}, \omega, \mathbf{G})\}\, d^2g. \qquad (19)$$

This comprises (i) a tone at the source frequency, whose directivity is equal to that of a plane interface, together with the attenuation factor (15) of a turbulent shear layer, and (ii) a series of refraction bands whose energy is spread continuously over a spectrum of frequencies $\omega_1 < \omega < \omega_2$ determined by the conditions $\mathrm{Re}(\gamma, \Gamma)$ (as for the diffraction by turbulence, §2.2) and which resemble (11) but with different amplitude and broadening functions Λ_n and Ω_n. Since in general $Q \propto \omega^2$ and $\Lambda \propto \omega^2$, in the low frequency limit only the unattenuated tone remains [see §2.1, equation (7)], whereas in the opposite asymptotic limit of large ω all the energy is drawn from the spike of the incident wave and distributed into a broad band of frequencies [see §2.2, equation (11)]. Since $C < 1$ we have

$$\int_{-\infty}^{+\infty} I(\theta, \phi, \omega)\, d\omega < J_0(\theta, \phi),$$

and in the audible range the energy received at all frequencies in the refraction bands is a fraction of that which is drawn from the spike $\{1 - \exp(-Q)\}J_0$. This is a particular case of the general property (part 1, §4.3) of a turbulent and/or irregular shear layer transmitting in each direction less energy over all frequencies than would a plane interface devoid of turbulence placed between the same media. This statement applies only to those directions, defined by real $\gamma(\mathbf{G})$ and $\Gamma(\mathbf{G})$ with

$$\mathbf{G} = (\omega/c_0)(\cos\theta, \sin\theta\sin\phi),$$

into which a plane interface can radiate; a turbulent and/or irregular shear layer

satisfies similar conditions, i.e. real $\gamma(\mathbf{g})$ and $\Gamma(\mathbf{g})$, but in terms of each incident wave component, and thus can also radiate into the 'zone of silence' of a plane interface.

The audible broadening function Ω_n consists of analogous terms in the time delay z_0 and longitudinal (z_1) and transverse (z_2) separations, and may be expressed as a sum of squares of deviation functions:

$$\Omega_n(\mathbf{g}, \omega, \mathbf{G}) = \sum_{i=0}^{2} \{v_n^{(i)}(\mathbf{g}, \omega, \mathbf{G})\}^2, \tag{20a}$$

$$v_n^{(i)} \equiv \{\{\omega - \omega_0 - g_1 U + \alpha V(g_1 - G_1)\} L_0, (g_1 - G_1) L_1, (g_2 - G_2) L_2\}/2n^{\frac{1}{2}}U. \tag{20b}$$

Since the broadening function appears as an exponential of negative argument in (19), the width of the spectrum scales inversely on $(2\pi)^3$ times the square of the refraction length per wavelength or refraction time per wave period, i.e. the spectrum is broader the more significant are the effects of scattering and diffraction. The audible amplitude function is given by

$$\Lambda_n(\mathbf{g}, \omega, \mathbf{G}) = (K|S|/A\gamma)^2 Q^n \exp(-Q) \prod_{i=0}^{n} L_i B_n(v_n^{(i)}), \tag{21a}$$

$$B_n(v) \equiv n^{-\frac{1}{2}} \sum_{r=0}^{n} \{(2n)^r (n-r)! r!\}^{-1} H_{2r}(v). \tag{21b}$$

Noting expression (15) for the attenuation factor, it is seen that the fraction of the energy received in each direction which is contained in the nth-order band scales on the nth power of the product of the square of the thickness of the shear layer and the r.m.s. height of irregularities measured on the scale of a wavelength, i.e. the intensity of the broad bands is greater relative to the spike the thicker and more irregular the shear layer is. The breadth and the amplitude of the spectral bands both depend on the deviation functions, which are defined by (20b), and vanish only for the component of the incident field that is transmitted without deflexion $(\mathbf{G} = \mathbf{g})$ and with unchanged frequency $(\omega = \omega_*)$, i.e. the component which corresponds to the spike. The formation of the bands is thus described by $v \neq 0$ and their shape depends on the side-band amplitude functions $B_n(v)$. The latter would be identically equal to unity $(B_n = 1)$ for an 'autocorrelation coefficient' of the form

$$E_*(z_i) = \prod_{i=0}^{2} \exp\{-(z_i/L_i)^2\},$$

corresponding to a convex 'hump' shaped band. The expression (21b), which involves Hermite polynomials $H_{2r}(v)$, is determined by the autocorrelation coefficient (9), which becomes negative beyond certain separations, this in turn having been observed experimentally and being associated with the conservation of the volume occupied by the jet (part 1, § 4.2). The first-order amplitude $\Lambda_1 = O(v^2)$, accordingly there is a dip at $v = 0$, i.e. near the spike; the bands of higher order $(n > 1)$ have terms $O(1)$ and partially fill the aforesaid dip. Since the bands must ultimately decay because of the exponential term in (19), the spectrum will exhibit side maxima, i.e. appear as a spike flanked by two side bands (see audible range in figure 1a).

The main theoretically predicted features of spectra both in the low and high frequency limits and in the audible range have been sketched in figure 1 (a), and may be summarized as follows: (i) scattering of a tone of low frequency incident upon an interface with a steady undulating shape gives rise to a transmitted tone at the

fundamental frequency which is flanked by a series of weaker tones (convection harmonics) if the undulations are convected relative to the source; (ii) diffraction of a high frequency tone by a thick layer of turbulence results in all the incident energy being spread over a continuous, convex transmitted broad band with maximum at the source frequency; (iii) a tone of frequency within the audible range incident upon a shear layer with an unsteady irregular shape and containing distributed turbulence is transmitted as an attenuated spike at the fundamental frequency, some of the remaining energy being transferred into side bands, which feature maxima, form a dip about the spike and decay smoothly outwards.

3. The description of a simple shear layer

The techniques used to evaluate the refraction integrals exactly or to obtain more accurate approximations might be of some interest in other branches of wave theory, and are thus described starting from a slightly more general mathematical form. The broad-band and side-band integrals that result can be evaluated explicitly in the case of a simple layer that nevertheless retains all the features essentially associated with the phenomenon of spectral broadening. The underlying picture of an array of re-radiating elements, each responsible for a line in the spectrum, shows how the complete sound field may be constructed via multinomial expansions of Hermite polynomials in the scattering–diffraction series.

3.1. *Evaluation of the refraction integrals*

The integral (18) is a special case, with $v \equiv g - G$ and $p(z/L) = 1 - 2z^2/L^2$, of the nth term of a power-series expansion in $p(z/L)$ of the general refraction (diffraction or scattering) integral

$$J(v, L, \mu) = \int_{-\infty}^{+\infty} \exp\{ivz - \mu[1 - p(z/L)\exp(-z^2/L^2)]\}\,dz \qquad (22)$$

featuring a phase v and attenuation μ. There is an effect of interference $\exp(\mu E)$, where E denotes the autocorrelation coefficient taken in the general form (part 1, §4.2) $E(z/L) = p(z/L)\exp(-z^2/L^2)$, in which the exponential shows that the correlation becomes negligible for separations larger than the refraction scale ($z > L$) and the polynomial factor $p(z/L)$ can be used to specify mean, symmetry, skewness or other properties. To evaluate (22) the constant attenuation $\exp(-\mu)$ may be taken out of the integrand and the exponential expanded in powers of $E(z/L)$, the zero-order term giving a delta function $\delta(v)$. Each higher-order term appears as an integral involving $\{E(z/L)\}^n$ with $n \geq 1$, and can be reduced to a Gaussian integral, of exponential argument $ivz - nz^2/L^2$, if we note that each factor z within the integrand is equivalent to $\partial/\partial(iv)$, e.g. $p(z/L)$ leads to $p\{\partial/\partial(ivL)\}$. Thus we obtain the scattering–diffraction series

$$J(v, L, \mu) = \exp(-\mu)\left\{2\pi\delta(v) + L\pi^{\frac{1}{2}} \sum_{n=1}^{\infty} \frac{\mu^n}{n!} P_n \exp(-v^2)\right\}, \quad v \equiv vL/2n^{\frac{1}{2}}, \quad (23a)$$

which introduces the side-band polynomials P_n defined by

$$P_n(v) \equiv \frac{\exp(v^2)}{n^{\frac{1}{2}}}\left\{p\left(\frac{-i}{2n^{\frac{1}{2}}}\frac{d}{dv}\right)\right\}^n \exp(-v^2), \quad H_r(v) \equiv (-1)^r \exp(v^2)\frac{d^r}{dv^r}\exp(-v^2),$$

$$(23b,c)$$

which in turn can be expressed via a multinomial expansion in terms of Hermite (1864) polynomials, which are defined (Courant & Hilbert 1966, p. 91) by (23c), with $r = 1, ..., nm$, where m is the degree of $p(z/L)$. The solution (23a) may be interpreted as an attenuated tone and a series of interference bands; noting that the exponential dominates the polynomial, $|P_n \exp(-v^2)| < b$ say, the series cannot exceed

$$\pi^{\frac{1}{2}} b (\exp(\mu) - 1),$$

and therefore is absolutely and uniformly convergent. If the bound b satisfies $b < 2\pi^{\frac{1}{2}}$ the interference bands contain, at most, energy $2\pi(1 - \exp(-\mu))$, which is refracted from the incident tone; otherwise, if $b > 2\pi^{\frac{1}{2}}$ the sum of the series could exceed the attenuation of the tone, in which case energy would have to be drawn from the refracting medium into the spectral bands.

The refraction series (23a) can be approximated by the first term for weak diffraction (Rayleigh 1915) with an error $O(\mu^2)$, or summed to any desired accuracy (Beckmann & Spizzichino 1963); for strong scattering $\mu \gg 1$, however, and convergence is slow (viz. no faster than the series for $\exp \mu$), requiring the summation of at least $N \sim 2\mu$ terms in order to give an acceptable accuracy. A convenient asymptotic estimate of (22) for $\mu \to \infty$ and when the polynomial p consists even powers only, i.e.

$$p(z/L) = p_0 - p_2(z/L)^2 + O(\{z/L\}^4),$$

involves a Gaussian integral for which the argument of the exponential is

$$ivz - \mu(p_0 + p_2)(z^2/L^2) + O(z^4/L^4),$$

and gives

$$J(v, L, \mu) = L\{\pi/q\}^{\frac{1}{2}} \exp\{-\mu(1 - p_0)\} \exp\{-v^2 L^2/4q\} + O(L^4 q^{-2}), \tag{24}$$

where $q \equiv \mu(p_0 + p_2)$ and the standard approximation ($O(q^{-1})$; see Jeffreys & Jeffreys 1946, p. 507) is improved to $O(q^{-2})$, or compared with the main term, improved from $O(q^{-\frac{1}{2}})$ to $O(q^{-\frac{3}{2}})$. This is a particular case of the asymptotic evaluation of integrals in which the amplitude is harmonic and the phase is stationary with next power $2s$ ($s > 1$), i.e. of the form

$$H(v, L, \mu) = \int_{-\infty}^{+\infty} \exp\{ivy - \mu y^2 + O(y^{2s})\} \, dy. \tag{25}$$

This is essentially a Gaussian integral, equal to $\{\pi/\mu\}^{\frac{1}{2}} \exp(-v^2)$ with $v \equiv \nu/2\mu^{\frac{1}{2}}$, with a correction $O(y^{2s}) = O(\{\partial/\partial(iv)\}^{2s}) = O(\{(4\mu)^{-1}\partial^2/\partial v^2\}^s)$:

$$H(v, L, \mu) = \{\pi/\mu\}^{\frac{1}{2}} \exp(-v^2/4\mu) + O(\mu^{-s}). \tag{26}$$

This proves (24), for which $s = 2$ (and $\mu \equiv q/L^2$), and also the statement made in §2.2 concerning the $O(\mathscr{L}^4)$ accuracy of the asymptotic estimate (11), where $\mu \equiv \mathscr{L}^{-2}$; all of the results (11), (24) and (26) represent smooth, convex broad bands. Our conclusions on the mathematical theory of refraction can be summarized in three brief statements: (i) the general refraction integral (22) can be evaluated exactly as a spike plus a side-band series (23a), using also (23b); (ii) the stationary-phase refraction integral (25) is given asymptotically for large attenuation by (26); (iii) if (ii) is applied to (22) with p an even polynomial the asymptotic estimate (24) follows.

These methods reduce the scattering or diffraction problem to the evaluation of spectral broad bands (11) or side bands (19), i.e. to multi-dimensional integrals over finite spectra. These integrals may be computed by means of a Monte Carlo method

(Hammersley & Handscomb 1960) which expresses them as the area of the wave-vector surface of integration D multiplied by the arithmetic mean of the integrand at N points taken randomly in D:

$$G(\mathbf{G}, \omega) = \int^{\mathrm{Re}\,(\gamma,\,\Gamma)} \Lambda(\mathfrak{g}, \omega) \exp\{-\Omega(\mathfrak{g}, \omega, \mathbf{G})\}\, d^2 g$$

$$\simeq \{|D|/n\} \sum_{q=0}^{n} \Lambda_q \exp(-\Omega_q) \simeq \{|\bar{D}|/N\} \sum_{q=0}^{n} \Lambda_q \exp(-\Omega_q) + O(n^{-\frac{1}{2}}). \quad (27\,a\text{–}c)$$

The domain D is defined by the condition that γ and Γ be real, and depends on $\mathfrak{g}$; it may be replaced by a fixed covering region $\bar{D} \equiv UD$, the integrand being set to zero for points in $\bar{D} - D$ (cf. Howe 1976). In the latter case we should need $N > n$ points from a statistically uniform distribution, so that $N/|\bar{D}| = n/|D|$, in order to obtain n points in D, the latter alone determining the accuracy of the calculation. The broadband and side-band integrals for the shear layer appear as products of three independent one-dimensional integrals, each with an integrand involving a term of the form (Lighthill 1958, p. 17)

$$\lim_{L \to \infty} (\pi/n)^{\frac{1}{2}} L \exp\{-(g - G)^2 L^2/4n\} = 2\pi\delta(g - G). \quad (28)$$

Thus, if one refraction scale is infinite, i.e. the medium is independent of time or uniform in some direction, the delta function in the expression (28) allows the corresponding integral with respect to g to be evaluated trivially.

3.2. *An array of re-radiating elements*

Consider a simple shear layer defined to be statistically independent of time and uniform in the direction (x_2) transverse to the mean flow, so that $L_0, L_2 \to \infty$, though longitudinal irregularities and turbulent perturbations remain with $L \equiv L_1 < \infty$. Introduction of the former conditions into (20) and (21) gives, by use of (28),

$$\delta(\omega - \omega_0 - g_1 U + \alpha V(g_1 - G_1))\, \delta(g_2 - G_2),$$

which allows the integration with respect to $\mathfrak{g}$ in (19) to be performed trivially, if $0 \neq (\partial\omega/\partial g_1) = \alpha V - U = c_0 M_r$, where $M_r \equiv \alpha M - M_0$. Thus spectral broadening occurs provided that the interface convects relative to the source $(M_r \neq 0)$, and the condition $\omega - \alpha V G_1 = \omega_0 - (\alpha V - U) g_1$ can be written in the form

$$\omega(1 - \alpha M \cos\theta) = \omega_0\{(1 - \alpha M \cos\theta')/(1 - M_0 \cos\theta')\},$$

where θ' is the local transmission angle (between the wave vector $(\mathfrak{g}, \Gamma)$ and the shear-layer mean plane $x_3 = 0$, i.e. $\tan\theta' = \Gamma/g$). The received frequency ω, normalized with regard to ω_*, that of the source, is given by

$$w(\theta, \theta') \equiv \frac{\omega}{\omega_*} = \frac{1 - M_0 \cos\theta}{1 - M_0 \cos\theta'} \frac{1 - \alpha M \cos\theta'}{1 - \alpha M \cos\theta} \quad (29)$$

and is a combination of Doppler factors associated with the source motion M_0, the shear-layer convection αM, the local transmission angle θ' and the observation angle θ in the far field. Expression (29) shows that each frequency of the received spectrum is emitted by a local radiating element which may be identified by the angle of transmission towards the observer θ'. The element radiating along the line $\theta = \theta'$ from

observer to source transmits the original tone $\omega = \omega_*$, while forward elements $(\theta' < \theta)$ re-radiate at lower frequencies $\omega < \omega_*$ and rearward ones $(\theta' > \theta)$ at higher frequencies $\omega > \omega_*$. This assumes that the Mach number of convection of the shear layer is larger than the source Mach number $(\alpha M > M_0)$; in the opposite case the frequency shifts would be interchanged between forward and rearward elements, leaving only the element along the line from the observer to the source to transmit at the (unchanged) fundamental frequency.

The locally incident (g, γ) and transmitted (g, Γ) wavenumbers in the horizontal (x_1) and vertical (x_3) directions are given by

$$(g, \gamma, \Gamma, k) = k_0 (1 - M_0 \cos \theta')^{-1} \{\cos \theta', \sin \theta', \psi(\theta'), \chi(\theta')\}, \tag{30a}$$

$$\chi(\theta') \equiv \{\cos^2 \theta' + [\psi(\theta')]^2\}^{\frac{1}{2}}, \quad \psi(\theta') \equiv \{(c_0/c)^2 (1 - M \cos \theta')^2 - \cos^2 \theta'\}^{\frac{1}{2}}, \tag{30b, c}$$

in which $k_0 = \omega_0/c_0$ and $k = \{g^2 + \gamma^2\}^{\frac{1}{2}}$ is the locally incident wavenumber. The horizontal wavenumber g is conserved across every re-radiating element, but the vertical wavenumber is continuous $(\gamma = \Gamma)$ only across the element defined by $\sin \theta_s = \psi(\theta_s)$, which transmits the incident wave without deflexion:

$$\theta_s = \cos^{-1} \{(1 \pm c/c_0)/M\}. \tag{31}$$

If the jet and the ambient medium have the same speed of sound $(c = c_0)$ the non-deflecting element lies on the vertical from the observer, $\theta_s = \frac{1}{2}\pi$; it exists provided that $1 + M \geqslant c/c_0 \geqslant 1 - M$ and lies in the forward arc if $c > c_0$ and in the rear arc if $c < c_0$, the displacement away from the vertical being smaller for higher Mach numbers. In order for undeflected transmission to occur $\psi(\theta_s)$ must be real, and this condition, in the general form $\mathrm{Re}\{\psi(\theta')\} \neq 0$, specifies the wave modes propagating from the jet into the ambient medium. The zeros of $(30c)$, which are given by $\psi(\theta_\pm) = 0$, viz.

$$\theta_\pm = \sec^{-1} (M \pm c/c_0), \tag{32}$$

define the angles at which total internal reflexion within the jet first occurs, and where the zones of silence begin; the latter are $\theta < \theta_+$ in the rear arc and $\theta > \pi - \theta_-$ in the forward arc. Rear and forward zones of silence occur respectively for jet Mach numbers $M > 1 \mp c/c_0$, i.e. a rear-arc zone of silence exists whenever the speed of sound in the jet is higher than that in the ambient medium. If a zone of silence exists in the forward arc then a larger one must be present in the rear arc, e.g. for identical media $(c = c_0)$ the forward silent arc starts at $M = 2$, when the rear zone of silence occupies a $70\cdot5°$ sector.

Since an incident beam tends to be sharpened when transmitted to the rear arc and to fan out in the forward arc, the field should be stronger in the former region. This statement is quantified by the transmission factor, which specifies the amplitude change associated with scattering by an interface, and is given by $|T| = 2/(1 + a)$, where $1 + a = A$ in $(2d)$. Thus

$$a(\theta') = (\rho c/\rho_0 c_0) \{(1 - M \cos \theta')/(1 - M_0 \cos \theta')\} \{\sin \theta'/\psi(\theta')\} \tag{33}$$

shows that the non-deflecting element between a jet and an ambient medium consisting of the same substance preserves the magnitude of the field ($a = 1$ for $\theta' = \frac{1}{2}\pi$ and $c = c_0$, $\rho = \rho_0$). For $\theta' = \frac{1}{2}\pi$ we have in general $T = 2\rho_0 c_0/(\rho c + \rho_0 c_0)$, viz., for perfect gases with the same molecular structure $\rho_0 c_0^2 = \rho c^2$, we have $T = 2c/(c + c_0)$,

which shows that the amplitude of the sound field is locally reduced if $c_0 > c$ and increased if $c > c_0$. The transmission factor modifies at each re-radiating element the amplitude of the wave emitted by the source, whose multipolar factor is given by $(2c)$, e.g.

$$S_0(\theta') = 1, \quad S_1(\theta') = \mathcal{M}\psi(\theta'), \quad S_2(\theta') = \mathcal{M}^2\{\{\psi(\theta')\}^2 + \cos^2\theta'\}, \qquad (34a\text{-}c)$$

where $\mathcal{M} \equiv (1 - M_0\cos\theta')^{-1}$, respectively, for (cf. Lighthill 1952, 1962) an omni-directional source (monopole S_0), an applied 'force' (vertical dipole S_1) and a (compressive) turbulent stress (quadrupole S_2). Formulae (30)–(34) apply in terms of θ to a plane interface and are also valid locally (in terms of θ') for an irregular and unsteady interface whose radius of curvature is (at all times) large on the wavelength scale. The latter condition is known as the Kirchhoff scattering approximation, and is expressed for random interfacial irregularities of r.m.s. height a and correlation length L by

$$(kL/8\pi)^2\{1 + (L/4a)^2\} \gg 1, \quad |\tan\theta_*| = \pi 2^{\frac{1}{2}}a/L, \qquad (35a,b)$$

where θ_* specifies the local r.m.s. slope. For a plane interface waves can be transmitted at angles θ satisfying $\theta_+ < \theta < \pi - \theta_-$, whereas for an irregular interface we exclude (when computing the spectra whose plots are to be shown subsequently, besides $\theta' < \theta_+$ and $\theta' > \pi - \theta_-$) waves radiated at grazing angles, i.e. below the mean slope of the interface ($\theta' < \theta_*$ or $\theta' > \pi - \theta_*$), which are re-scattered in other directions and constitute a diffuse field. The latter is weak if the interfacial irregularities are shallow ($L^2/4a^2 \gg 1$), in which case Kirchhoff's scattering theory applies to wavelengths smaller than or of the order of magnitude of the correlation length ($\lambda \lesssim L$).

3.3. Scattering–diffraction series expansion

The degenerate case of the array of local radiating elements is furnished by a plane interface which transmits sound at the same frequency as the source with directivity (5), given in the fly-over plane $\phi = 0$ by

$$J_0(\theta) = (8\pi^2\rho_0 c_0)^{-1}\{\sin^2\theta/(1 - M_0\cos\theta)\}\{S(\theta)/A(\theta)\,\psi(\theta)\}^2. \qquad (36)$$

For identical media at rest $\psi(\theta) = \sin\theta$, $A(\theta) = 1$ and (36) simplifies to

$$\{S(\theta)\}^2/\{8\pi^2\rho_0 c_0(1 - M_0\cos\theta)\},$$

but the amplitude is modified by propagation within the jet and transmission to the ambient medium, being singular only on the Mach cone $\cos\theta = 1/M_0$ in the supersonic case (the cone degenerating into a plane in the sonic case). Even if we regard each local re-radiating element of the model array as being plane, it will emit sound at its own characteristic frequency, which is given by (29), replacing the directivity $J_0(\theta)$ of a plane interface by a simple layer function defined as

$$J_*(\theta, \theta') = \frac{(1)^{-1}/\rho_0 c_0 \sin^2\theta/c_0 M_r}{16\pi^{\frac{5}{2}}1 - M_0\cos\theta} \cdot \left[\frac{1 - \alpha M\cos\theta'}{1 - \alpha M\cos\theta}\frac{S(\theta)}{\psi(\theta')A(\theta')}\right]^2, \qquad (37)$$

which is related to the former [see (36)] by $J_*(\theta, \theta) = J_0(\theta)/(2\pi^{\frac{1}{2}}c_0 M_r)$. Here the factor $2\pi^{\frac{1}{2}}$ implies that we are considering one finite refraction scale (parallel to the mean flow in the shear layer) to account for both the scattering by longitudinal irregularities of the interface and diffraction by turbulence with velocity perturbations lying in the plane $\phi = 0$ (which is specified by the velocity of the jet and the observer position in

the ambient medium), and accordingly the factor $c_0 M_r$ is associated with the occurrence of spectral broadening (§ 3.2).

Thus one property absent in the refraction by a plane interface but relevant to our simple shear layer model is spectral broadening, which is expressed by the function Ω_n. This is identically zero in the former case $(\Omega_n(\theta, \theta) = 0)$ and from $(20a)$ is given at each re-radiating element by

$$\Omega_n(\theta, \theta') \equiv \{v_n(\theta, \theta')\}^2 = \frac{k_0^2 L^2}{4n} \left[\frac{\cos\theta - \cos\theta}{(1 - M_0 \cos\theta')(1 - \alpha M \cos\theta)}\right]^2 \tag{38}$$

for an irregular and/or turbulent shear layer. In the latter case the spectral broadening function Ω_n vanishes only for the radiating element on the line from observer to source $(\theta = \theta')$, which is the one transmitting the original tone; higher and lower frequencies are affected by the term $\exp(-\Omega_n)$ that limits the energy contained in the outer regions of the spectrum. The deviation function $v_n(\theta, \theta')$, which is given by (38), specifies (besides Ω_n), by means of $(21b)$, the side-band amplitude function:

$$B_n(\theta, \theta') = n^{-\frac{1}{2}} \sum_{r=0}^{n} \{(2n)^r (n-r)! \, r!\}^{-1} H_{2r}\{v_n(\theta, \theta')\}, \tag{39}$$

in which the Hermite polynomials H_{2r} may be calculated from the definition $(23c)$ or the recurrence formula $H_{n+1}(v) = 2vH_n(v) - 2nH_{n-1}(v)$ (Courant & Hilbert 1966, p. 92), e.g. $H_0 = 1$, $H_2 = 4v^2 - 2$ and $H_4 = 16v^4 - 48v^2 + 12$. In the first-order refraction $B_1 = \theta_1^2 = 2\Omega_1$, and this implies the appearance of a dip in the spectral broad band, corresponding to transmitted sound with $v_1 = 0 = \Omega_1$, i.e. centred at the spike, which is thus flanked by two side bands. Higher-order terms, e.g. $B_1 = \frac{3}{8} - \frac{1}{2}v^2(1-v^2)$ with $v \equiv v_1$, partially fill in the dip and augment the side bands; the subsequent terms $\Omega_n = O(1/n)$ correspond to wider convex bands, spreading outwards, so that the spectrum tends to fall off linearly or with a slightly concave shape (on a logarithmic scale) from the side-band maxima.

Another property of the simple shear layer is attenuation of sound, which is expressed from (15) by means of the attenuation factor

$$Q(\theta') = \mathcal{M}^2\{k_0^2 a^2\{\psi(\theta') - \sin\theta'\}^2 + \beta^2 M^2\{\chi(\theta')\}^2 b^2 \operatorname{cosec}\theta'\}, \tag{40}$$

which consists of two terms associated with (i) scattering by interfacial irregularities of r.m.s. height a, which reduces re-radiation from each element the further it lies from the non-deflecting element given by $\psi(\theta_s) = \sin\theta_s$ [see (31)] and which defines the only angle for which energy is conserved, and (ii) diffraction by a region of turbulence in the shear layer of effective thickness b that involves attenuation at *all* re-radiating elements (e.g. $Q_s = \beta^2 M^2 b^2 \operatorname{cosec}\theta_s$ at the non-deflecting element), the degree of attenuation increasing as the angle of incidence approaches grazing directions, for which the ray paths are longest. The effects of attenuation are included explicitly in the expression (19) for the audible spectral directivity, which in the case of refraction by a simple shear layer takes the form

$$I(\theta, \theta') = J(\theta, \theta') \exp\{-Q(\theta')\}\{2\pi^{\frac{1}{2}}c_0 M_r \, \delta(\theta - \theta')$$

$$+ \sum_{n=1}^{\infty} \{Q(\theta')\}^n B_n(\theta, \theta') \exp\{-\Omega_n(\theta, \theta')\}. \tag{41}$$

The first two factors on the right are respectively the simple layer function (37) and

the directional attenuation exponential specified by (40), thus the transmitted sound field is made up of two components: (i) a tone refracted by the re-radiating element in the line of sight from the observer to the source; (ii) a scattering–diffraction series expansion, consisting of interference bands defined by (38) and (39) of orders $n \geqslant 1$, re-radiated by all other (offset) elements of the model array.

In order to obtain the spectrum received in a given observation direction θ, we may scan all re-radiating elements lying in the angular range

$$\theta_1 \equiv \sup(0, \theta_+, \theta_*) < \theta' < \inf(\pi - \theta_*, \pi - \theta_-, \pi) \equiv \theta_2$$

[see (33) and (35b)], their emission frequency being determined from (4b) and (29) by means of the expression $\omega(\theta, \theta') = \omega_*(\theta) w(\theta, \theta')$ in the spectral band

$$\omega_1 \equiv \omega(\theta, \theta_1) < \omega < \omega(\theta, \theta_2) \equiv \omega_2.$$

The corresponding received energy (viz. the audible spectral directivity) $I(\theta, \theta')$ is given by (41). If the observer is located in the rear arc ($\theta < \frac{1}{2}\pi$) the spectrum extends more into the frequencies higher than that of the source ($\omega_2 > \omega > \omega_*$), corresponding to $\theta < \theta' < \theta_2$, and less into the lower frequencies ($\omega_1 < \omega < \omega_*$), for which $\theta > \theta' > \theta_1$, i.e. $\omega_2 - \omega_* > \omega_* - \omega_1$; conversely, if the observer is located in the forward arc the spectral bands are biased towards the low frequencies. The series in (41) specifying the side bands must be summed to an accuracy of $\pm 0.3\%$, in order to correspond to the minimum level of distortion which is discernible to the human ear (15 dB), which perceives sound nearly logarithmically. Thus we represent the spectral directivity on a decibel scale (in figures 2–5), normalized to the maximum of (the higher of) the side bands $I_m(\theta)$, taken as the 15 dB reference for audible distortion:

$$\mathrm{II}(\theta, \theta') \equiv 15 + 10 \log_{10}\{I(\theta, \theta')/I_m(\theta)\}. \tag{42a}$$

The directivity is defined as the energy received over all frequencies in a given direction and is normalized to the maximum energy J_m in the tone of a plane interface (36), which an irregular and/or turbulent shear layer cannot exceed (§ 2.3; also part 1, § 4.3). Thus J_m is taken as the reference level for

$$\mathrm{III}(\theta) \equiv 40 + 10 \log_{10}\left\{J_m^{-1} \int_{\theta_1}^{\theta_2} I(\theta, \theta')\, d\theta'\right\}, \tag{42b}$$

a dynamic (or total directivity) range of 40 dB being sufficient for the assessment of the audible disturbance of aircraft noise.

Some of the main effects of refraction of sound by a turbulent and irregular shear layer are summarized diagrammatically in figure 1 (b): a source convected within the jet emits monochromatic radiation to all re-radiating elements of the array which models a simple shear layer. Each re-radiating element transmits the incident tone in one direction (calculated as for a plane interface) as an attenuated spike, provided that the angle of total internal reflexion into the jet is not exceeded; some of the energy which is attenuated from the spike is re-emitted in all other directions, contributing an interval to the frequency band of the spectrum received at each off-set observer direction, except for grazing directions, for which multiple scattering occurs. For an observer lying on the vertical to the jet axis the model is symmetric except for the mean flow velocity, and thus the received spectrum is approximately symmetric

about the source frequency for low speed jets; for an observer located in the forward arc the radiation coming from the forward elements predominates and the spectrum is biased towards the low frequencies (and conversely in the rear arc).

4. Comparison of prediction and observation

In order to compare the present theory of spectral broadening with noise measurements of jets it is necessary to know fairly precisely the location and properties of sound sources, so that scattering and diffraction effects can be isolated; in this respect the experiments of Candel *et al.* (1975) appear to be the most appropriate collection of measurements concerning the transmission of sound through shear layers. When applying the theory to the prediction of the spectra at various angles to the axis of high speed jets we shall consider a tone of frequency 8–10 kHz typical of the order of magnitude of the rotation speeds of turbines (and compressors) of modern jet engines. If the agreement between theory and experiment which is exhibited at low jet speeds (figures 3 and 4) were to be maintained for high speed jets, then the prediction (figure 5) that a tone can be considerably attenuated, and its energy spread over a spectral band of several kilohertz, as a result of the scattering by irregularities and diffraction by turbulence of the shear layer (even if of small scale) gives some hope with regard to the reduction of the noise disturbance caused by sources located in the exhausts of jet engines.

4.1. *Experiments with sources in an open wind tunnel*

The spectra of test sources emitting monochromatic radiation which is refracted by turbulent and irregular shear layers were measured in two series of experiments performed by Candel *et al.* In the first (Candel, Julienne & Julliand 1975) the source was located on one side of a jet exhausting from a rectangular nozzle, the size of which ranged from 30×190 mm to 190×90 mm, placed within a wind tunnel, in order to simulate the shielding of noise by a double shear layer. The second series, by Candel, Guédel & Julienne (1975), concerned a source located in the interior of an axisymmetric jet exhausting from a circular nozzle of diameter 3000 mm into an anechoic chamber, for the ultimate purpose of developing methods of transposition of noise measurements taken in the exterior of a jet to its interior. Although the present theory applies to the former case of a double shear layer (part 1, § 3.2), the latter series of experiments is more representative of the transmission of noise from the interior of a jet, in both cases cold air at low speed. Thus we adopt the collection of measurements in Candel, Guédel & Julienne (1975), some of which (namely their figures 2, 4, 6 and $25a$–c) are reproduced in our figure 3 (a), for comparison with computations based on the present theory. The reference case is a low speed cold air jet containing a high frequency source:

$$V = 60 \, \text{m/s}, \quad c/c_0 = 1 = \rho_0/\rho, \quad f = 20 \, \text{kHz}, \qquad (43a\text{–}c)$$

the source being located at a station $X_0 = 500$ mm downstream of the nozzle (see their figure 4, reproduced in our figure 3a). Conditions ($43a$, c) were varied to consider, in all, three low jet speeds $V = 20$, 40 and 60 m/s, six high but audible frequencies $f = 4$, 6, 8, 10, 15 and 20 kHz and shear-layer scales at two stations $X_0 = 500$ and 1950 mm.
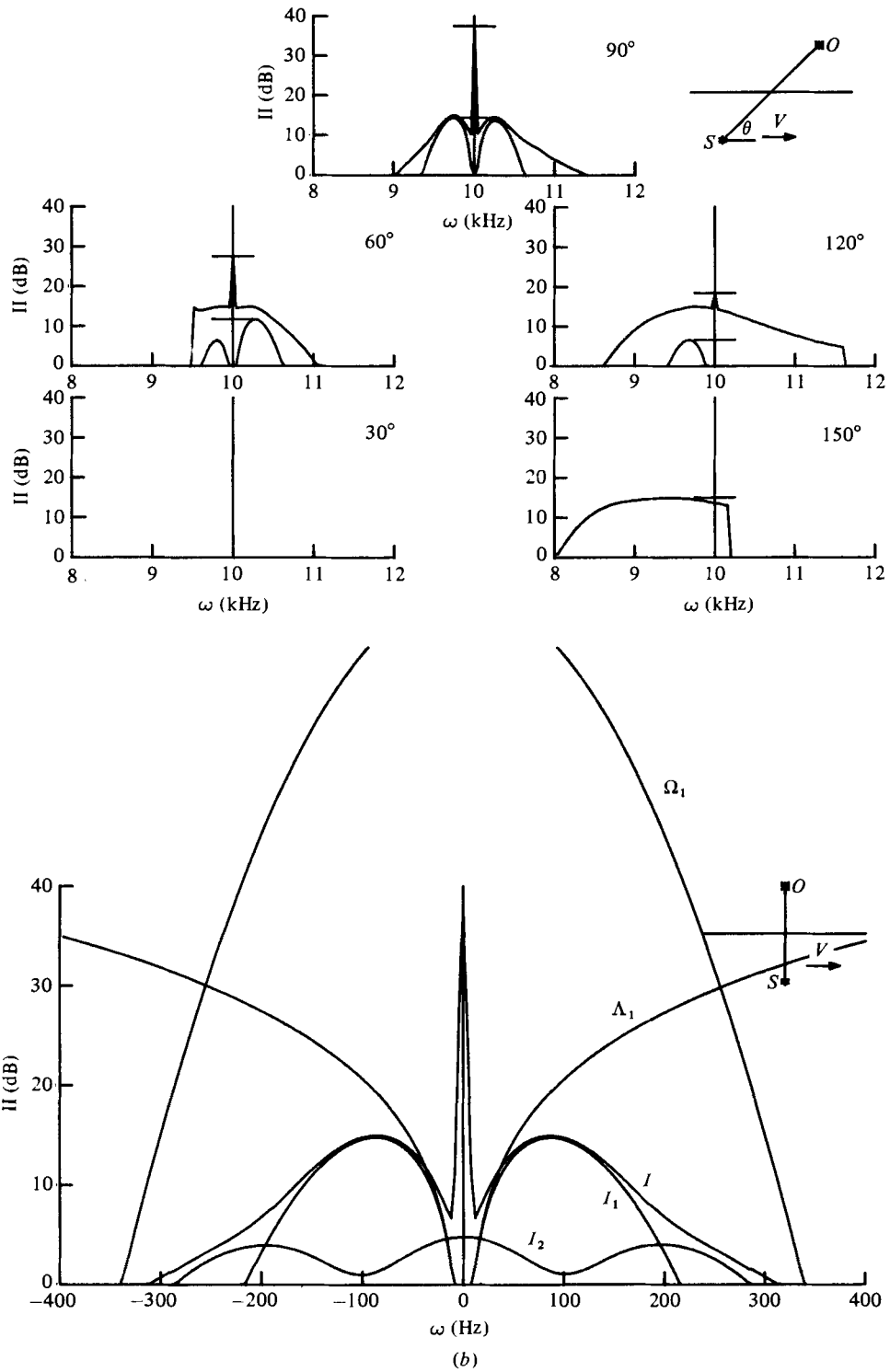
FIGURE 2. Modelling by computer program. (a) High-speed directional spectra; $M = 0.8$, $L = 200$ mm, $f = 10$ kHz, $d = 0.710$, $c = 0.934$, $b = 35$ mm, $a = 20$ mm. (b) Formation of a low speed spectrum.
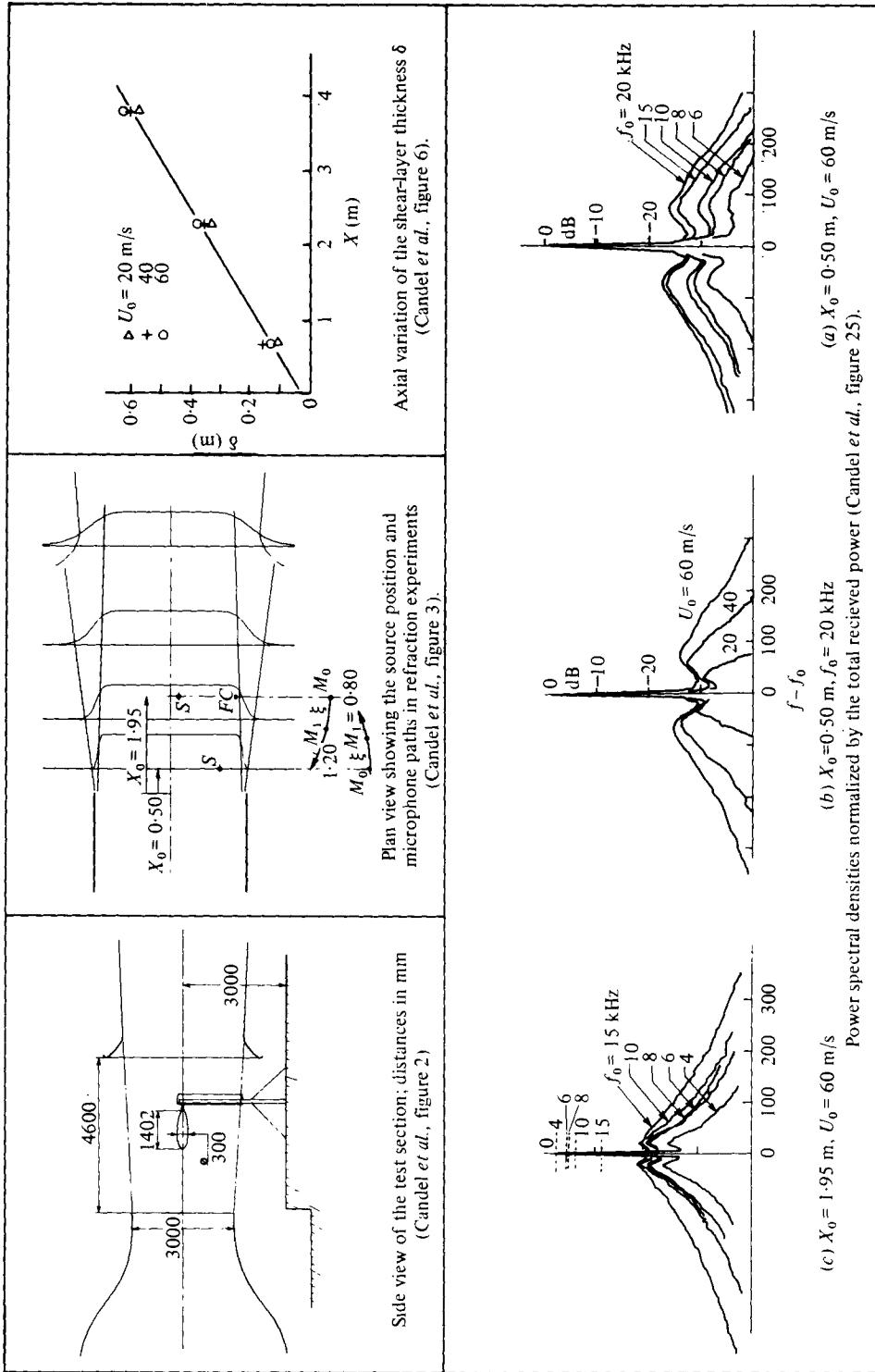
Side view of the test section; distances in mm
(Candel *et al.*, figure 2)

Plan view showing the source position and
microphone paths in refraction experiments
(Candel *et al.*, figure 3).

Axial variation of the shear-layer thickness δ
(Candel *et al.*, figure 6).

$(c) X_0 = 1.95$ m, $U_0 = 60$ m/s

$(b) X_0 = 0.50$ m, $f_0 = 20$ kHz

$(a) X_0 = 0.50$ m, $U_0 = 60$ m/s.

Power spectral densities normalized by the total recieved power (Candel *et al.*, figure 25).
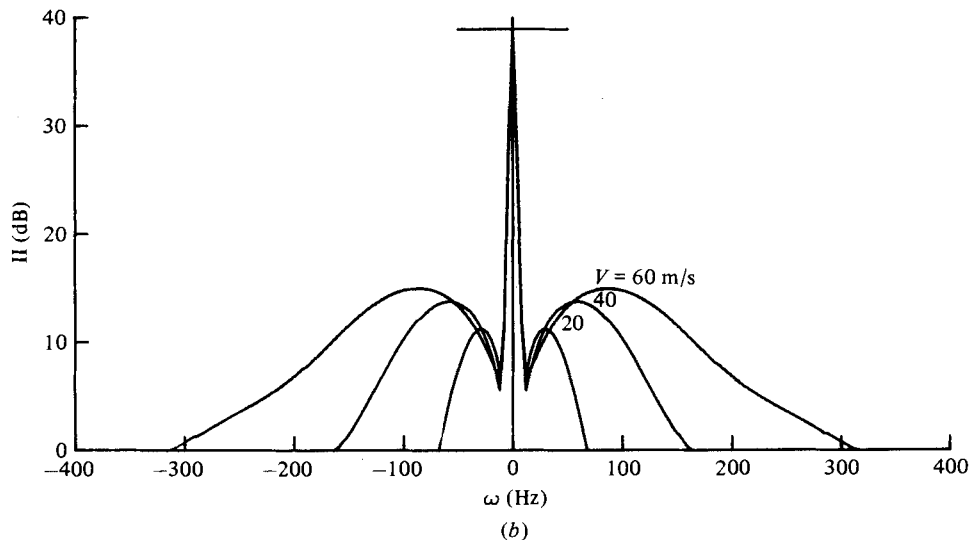
(a)

FIGURE 3(*a*). For legend see next page.

26-2

FIGURE 3. Influence of jet velocity. (a) Figures 2, 3, 6 and 25 from Candel, Guédel & Julienne (1975). (b) Plot of corresponding simulation; $\theta = 90°$, $M = 0·176$, $L = 135\,\text{mm}$, $f = 20\,\text{kH}$, $d = 1·000$, $c = 1·000$, $b = 55\,\text{mm}$, $a = 55\,\text{mm}$, monopole source.

The source of sound used in the experiments was a compression chamber enclosed in an aerodynamically shaped profile and radiating through a small lateral hole. The directivity pattern measured in the absence of flow is fairly complex, but this is of little consequence to the comparison of spectra, which were all measured in the same direction $\theta = 90°$ (perpendicular to the jet axis). The directivity pattern of emission will have no effect on the computed spectra if the source is assumed to be a monopole. Judging by their figure 6 (our figure 3a), the thickness of the shear layer at $X_0 = 500\,\text{mm}$ is about 110 mm, suggesting an r.m.s. height of irregularities of 55 mm, i.e. we take

$$S = 1, \quad a = 55\,\text{mm} = b, \quad L = 135\,\text{mm}, \qquad (44a\text{–}c)$$

in which L is the refraction scale. Our point of view is that a sample experimental spectrum could be used to determine the values of the parameters a, b and L that give the best fit with one computed spectrum; this is an example of the use of the knowledge of the distortion of a test tone to estimate the properties of the medium of propagation (part 1, §1.3). The values (44a–c) thus chosen should, of course, be retained for the computation of every spectrum measured at the same station, viz. in the present case eight distinct spectra. The first comparison of experimental measurements (their figure 25b, in our figure 3a) and the corresponding theoretical computation (figure 3b) concerns the effects of increasing the jet velocity. These are apparent as (i) a proportional increase in the width of the central dip between the maxima of the side bands, (ii) higher side-band maxima, implying that a larger fraction of the energy of the incident tone is transmitted in the side bands, and (iii) broadening of the range of frequencies occupied by the spectrum. The frequency and level of the side maxima, and the breadth of the spectrum are given in table 1, in which computed results are compared with the values which can be discerned from the small graphs in Candel, Guédel & Julienne (1975), the latter being given in parentheses.
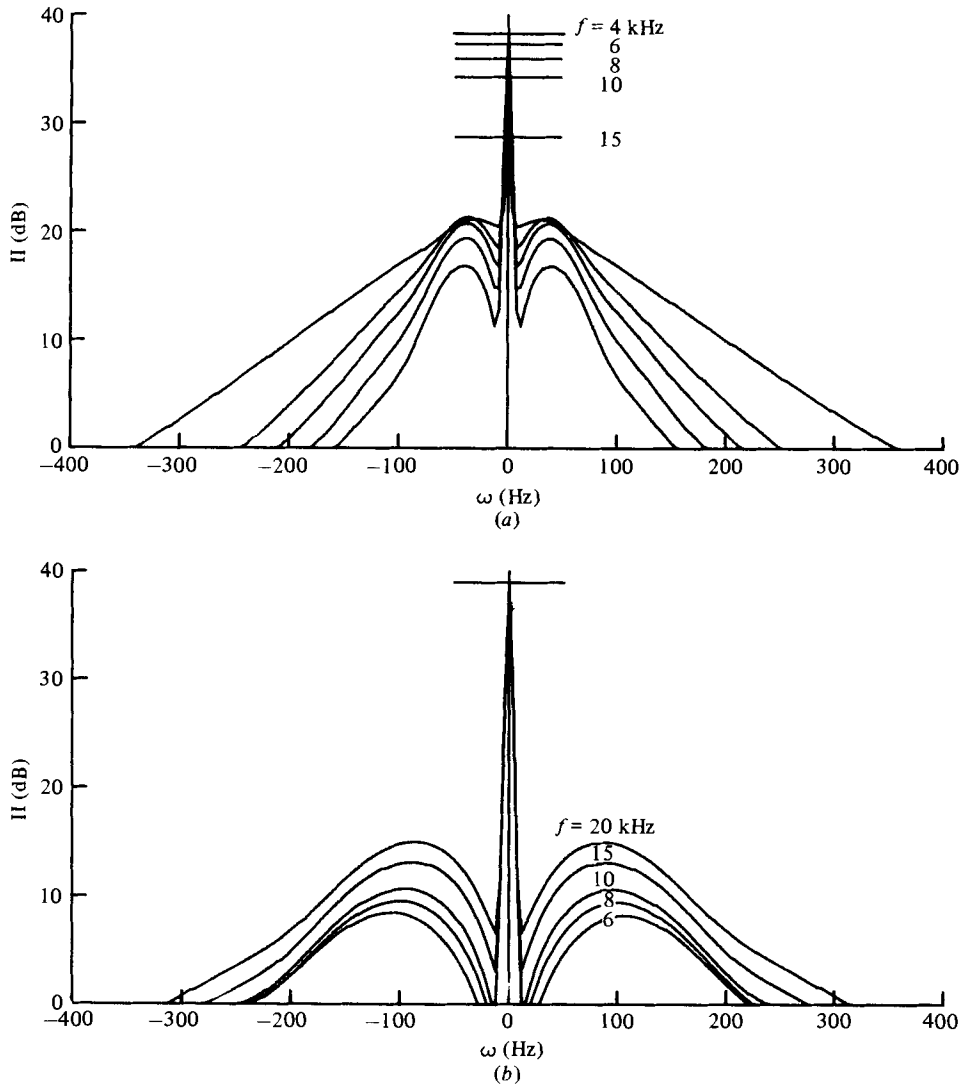
FIGURE 4. Effect of source frequency; $\theta = 90°$, $M = 0.176$, $d = 1.000$, $c = 1.000$, monopole source. (a) Developed turbulence downstream; $L = 300$ mm, $b = 217$ mm, $a = 110$ mm. (b) Thin shear layer near a nozzle; $L = 135$ mm, $b = 55$ mm, $a = 55$ mm.

Jet velocity (m/s)	(i) Dip width (Hz)	(ii) Maximum level (dB)	(iii) Side-band breadth (Hz)
20	28 (29)	11·3 (10·0)	67 (77)
40	58 (58)	13·8 (13·4)	162 (184)
60	86 (75)	15·0 (15·0)	313 (315)

TABLE 1

Source frequency (kHz)	Maximum level (dB)	Side-band breadth (Hz)
6	8·2 (4·4)	221 (171)
8	9·4 (7·7)	225 (232)
10	10·6 (10·0)	233 (232)
15	13·1 (13·6)	274 (280)
20	15·0 (15·0)	313 (315)

TABLE 2

Source frequency (kHz)	Maximum of side band (dB)	Breadth of side band (Hz)	Spike level (dB)
4	16·8 (15·3)	153 (130)	38·3 (38·0)
6	19·4 (19·0)	181 (197)	37·3 (36·0)
8	20·8 (19·8)	213 (215)	36·0 (35·5)
10	21·3 (20·7)	249 (238)	34·3 (34·0)
15	21·1 (21·2)	357 (350)	28·7 (29·0)

TABLE 3

According to the experimental results in figure 25 (a) of Candel, Guédel & Julienne (in our figure 3 a), which were obtained at the same station as before, and the corresponding theoretical prediction of figure 4 (b), increasing the frequency of the source increases the energy contained in the side bands, which exhibit higher maxima and also become broader. A detailed comparison gives the results presented in table 2.

The eight distinct spectra in tables 1 and 2 are for the same station $X_0 = 500$ mm, fairly close to the nozzle exit (axial distance/nozzle diameter $= X_0/\Delta = \frac{1}{6}$), where the shear layer is relatively thin [see (44)] and the attenuation effects are barely noticeable (i.e. < 1 dB). According to figure 5, the shear-layer thickness increases approximately linearly with the axial co-ordinate downstream (at least for distances of the order of a jet diameter), and at $X_0 = 1950$ mm (or $X_0/\Delta = 0.65$) the (effective) thickness of the turbulent shear layer should be taken as $b = 3.95 \times 55$ mm. The irregularities may increase more slowly in (r.m.s.) height and the turbulence intensity may be expected to become somewhat weaker in a broader layer, and the refraction scale larger. Accordingly at this station we take

$$a = 110\,\text{mm}, \quad L = 300\,\text{mm}, \quad b = 217\,\text{mm}. \tag{45a–c}$$

These values are used in the computation of the theoretical prediction in figure 4 a, which corresponds to the experimental measurements in figure 25 (c) of Candel, Guédel & Julienne (in our figure 3 a), showing that the central dip narrows considerably (to $\simeq 32$ Hz) but again the side bands are broader and higher as the source frequency increases; see table 3. If the spike attains 38·3 dB for a 4 kHz source tone, then a comparison with the energy transmitted at other source frequencies (namely 6, 8, 10 and 15 kHz) gives the spike levels indicated in table 3, showing the increase in attenuation of tones at higher frequencies caused by a thick and sinuous shear layer.

Station X_0/D	Jet velocity (m/s)	Source frequency (kHz)					
		4	6	8	10	15	20
⅛	20	–	–	–	–	–	*
⅛	40	–	–	–	–	–	*
⅛	60	–	*	*	*	*	†
0·65	60	*	*	*	*	*	–

TABLE 4

4.2. *Directional spectra for a high speed jet*

A monochromatic source of nominal fundamental frequency ω_* actually emits over a range of frequencies $\omega_* - \epsilon < \omega < \omega_* + \epsilon$, the width of which will be relatively small $(2\epsilon \ll \omega_*)$, thereby simulating a 'tone'. The distribution of the energy emitted by the source at each frequency in the range $(\omega_* - \epsilon, \omega_* + \epsilon)$ is given by some function $F(\omega)$, and is received as the spike whose shape is essentially unchanged during transmission through the shear layer, apart from an overall attenuation $\exp(-Q)$ of the directivity relative to that (J_0) of a plane interface. The total energy in the spike is given as the coefficient of the delta function on the right-hand side of (19), viz.

$$J_0 \exp(-Q) = \int_{\omega_* - \epsilon}^{\omega_* + \epsilon} F(\omega)\, d\omega,$$

e.g. for $F(\omega) \equiv f \times (1 - |\omega - \omega_*|/\delta)^p$ the height of the spike is equal to f and is determined by $f = \frac{1}{2}(p+1) J_0 e^{-Q}$. For the purpose of sketching the spike in the plots in figures 2–5 we have taken $p = 7$ and $\epsilon = \frac{80}{3}\pi$ (i.e. $\epsilon/2\pi = \frac{40}{3}$ Hz), the values assumed being of no consequence to the relative levels of spikes, which depend only on the ratio of the respective plane-interface directivities and the difference of shear-layer attenuations, according to $f_1/f_2 = (J_{01}/J_{02}) \exp(Q_2 - Q_1)$. Typically in the transmitted field the spike is flanked by side bands, the formation of which is illustrated in figure 2(b) for the conditions (43) and (44) corresponding to the reference case in the experiments of Candel, Guédel & Julienne (1975). The first-order side band I_1 is a result of amplification by interference between adjoining radiating elements Λ_1, dominated in the outer portions of the spectrum by the decay $\exp(-\Omega_1)$ associated with independent attenuation, which is more marked at shallow angles of incidence. The second-order term I_2 of the scattering–diffraction series expansion partially fills the dip centred at the spike, and also causes the side bands to extend further outwards, resulting in a nearly linear or slightly concave decay of the full spectrum I. A detailed comparison of the spectra obtained by the method of computation described above with those measured experimentally by Candel, Guédel & Julienne (1975) and illustrated in figures 3 and 4 exhibits encouraging agreement in the 13 distinct cases listed in table 4. We have marked with a dagger the reference case, corresponding to the values of the parameters indicated in (43) and (44), and emphasize that so far we have been concerned with (a monopole source immersed in) cold air jets of low subsonic speed, for which comparable measurements are available.

The theory is also applicable at other values of the jet Mach number M, source frequency f (in Hz) and of the ratios c and d, respectively, of the sound speeds and mass densities in the jet and in the ambient medium:

$$M = V/c_0, \quad c = c/c_0, \quad d = \rho/\rho_0, \quad f = \omega_0/2\pi. \qquad (46a\text{-}d)$$

These parameters may be adjusted to characterize various conditions, such as those in which full-scale measurements with test sources might be difficult to perform accurately, e.g. a high subsonic flow of a diatomic perfect gas (Landau & Lifshitz 1959, § 80) for which

$$M = 0.8, \quad c = 0.934, \quad d = 0.710 \qquad (47a\text{-}c)$$

and which contains a high frequency compressive quadrupole source, modelling sound produced by a turbulent eddy behind a thin shear layer. We assume

$$f = 10 \, \text{kHz}, \quad a = 20 \, \text{mm}, \quad b = 35 \, \text{mm}, \quad L = 200 \, \text{mm}, \qquad (48a\text{-}d)$$

i.e. a fairly small value for the r.m.s. height a of irregularities, a slightly larger one for the thickness b of the turbulent region and a refraction scale L corresponding to turbulence of moderate intensity, in order to show that spectral broadening is significant for most high speed jets. The complete spectra and the first interference band (i.e. the term I_1 of order $n = 1$ in the scattering–diffraction series expansion) have been plotted in figure 2(a) for conditions (46) and (47) for five directions spaced at 30° (viz. at angles $\theta = 30°, 60°, 90°, 120°, 150°$ in the 'fly-over' plane $\phi = 0$). The spectrum of the sound received at right angles to the jet is more asymmetrical than in figure 2(b) as a result of the high speed of the jet.

The asymmetry of the spectra becomes more apparent away from the vertical (i.e. $\theta = 90°$) direction and, as predicted in §3.3, for an observer in the rear arc ($\theta < 90°$) the spectrum extends further into frequencies higher than that of the source, whereas for an observer in the forward arc ($\theta > 90°$) the spectrum is biased towards the lower frequencies. Therefore, when listing in table 5 below the maxima and breadth of the overall side bands (and also, in brackets, the corresponding magnitudes for the first-order side band), we write the values corresponding to frequencies lower and higher than that of the source before and after the stroke, respectively, for the left/right spectral side bands. The first-order interference band is a poor approximation to the full side band for the spectrum at 90°, becomes a small contribution at 120°, and is negligible at 150°. Correspondingly, the calculation of the full side band to the specified accuracy of 15 dB below the maximum in each direction required 4–8 terms of the scattering–diffraction series at 90°, whereas 10–33 terms were necessary for the spectrum at 120°. These two statements illustrate the property that the interference between neighbouring re-radiating elements modelling scattering and diffraction by the turbulent and irregular shear layer are more significant (i) for each observer direction, for frequencies distant from the source frequency, and (ii) in general, for grazing directions of observation. The spike is progressively attenuated as the observer moves away from the vertical into the forward arc (e.g. at 120°; the spike subsides into the broad band at 150°), and is absent to the rear of $\theta_+ = 59.4°$, which is the angle of total internal reflexion calculated from (33) for a plane interface between media which are described by (47b).

Angle θ	Overall (first-order) side band		Peak level (dB)
	Maxima (dB)	Breadth (kHz)	
30°	$-\,/\,-$	$-\,/\,-$	—
	$(\,-\,/\,-\,)$	$(\,-\,/\,-\,)$	
60°	15·0/15·0	0·48/1·05	27·6†
	$(\,-\,/\,-\,)$	(0·39/0·62)	
90°	15·0/14·7	0·97/1·39	37·6†
	(14·4/13·8)	(0·65/0·62)	
120°	15·0/ $-$	1·37/1·60	18·4†
	$(\,-\,/\,-\,)$	(0·58/0·12)	
150°	15·0/ $-$	1·97/0·16	13·5‡
	$(\,-\,/\,-\,)$	$(\,-\,/\,-\,)$	

† Level at spike.   ‡ Level of band at source frequency (spike indiscernible).

TABLE 5

4.3. *Application to a jet-engine exhaust*

The dynamical model of the shear layer features two characteristic velocity coefficients, viz. the mean eddy convection velocity αV and the turbulent perturbation velocity $\mathbf{u} = \beta V\mathbf{m}$, for which we have taken at low Mach numbers (Barratt *et al.* 1963) $\alpha \simeq 0.6$ and $\beta \simeq 0.15$, values which remain approximately valid at high jet speeds. The Kirchhoff scattering approximation (35*a*) may be expected to be satisfied for high frequency sound ($k^2 L^2/4\pi^2 \gg 1$) incident upon an interface [see (35*b*)] with either shallow ($L^2/2\pi^2 a^2 \gg 1$) or moderately steep ($L \simeq 2^{\frac{1}{2}}\pi a$) irregularities, and the local turbulence (part 1, §2.2) would remain effectively incompressible if $(\beta Mc_0/c)^2 \ll 1$, i.e. (since $\beta \simeq 0.15$) for supersonic jets satisfying $M \lesssim 2c/c_0$. The present shear-layer model is expected to apply to shock-free refraction by moderately supersonic flows; shock waves resemble interfaces in that they appear as surfaces of discontinuity of density (and sound speed). However, the pressure also changes across a shock wave, unlike an interface, and the discontinuity in the mean velocity is normal in the former and tangential in the latter cases. The system of shock cells in a supercritical jet lies behind the interface, the irregularities of which can also produce shocks, and either set of shock waves could interact with the turbulence adjoining the interface. We make the admittedly rather simplistic assumption that all localized scattering and distributed diffraction effects can be modelled by means of three possibly modified statistical scales of the shear layer, namely the (r.m.s.) height a of the interfacial irregularities, the (effective) thickness b of the region of turbulence and the (longitudinal) refraction length L. As a practical application, in order to have an idea of the significance of spectral broadening in the difficult but important case of Concorde at take-off, we assume the following shear-layer scales:

$$a = 40, 80 \text{ mm}, \quad L = 125 \text{ mm}, \quad b = 50, 100 \text{ mm}, \qquad (49a\text{--}c)$$

the second set of values corresponding to a shear layer of double thickness and irregularity, for which greater attenuation of noise emitted within the jet might be expected.

The exhaust gas of the (Rolls-Royce/SNECMA) Olympus (593D Mk. 612 twin-spool turbojet) engine which powers (the production series) Concorde is thermodynamically imperfect, and the hot, low density flow is supersonic compared with the atmospheric sound speed. The take-off, noise abatement and climb thrust ratings correspond to exhaust properties which differ in detail, but the following values are representative as orders of magnitude:

$$M = 2\cdot0, \quad c = 1\cdot8, \quad d = 0\cdot3, \quad f = 8\,\text{kHz}. \qquad (50a\text{–}d)$$

As an illustration we shall consider a vertical dipole source whose frequency we take to be 8 kHz, corresponding to the rotation speed of the high pressure compressor-turbine assembly, and hence to the turbine tone associated with mechanically induced vibration. Although the turbine tone is emitted within the engine nacelle, it can be modelled by a distribution of monopoles and dipoles in the nozzle exit plane; at supersonic flow velocities these sources can only radiate downstream, precluding any significant effect of scattering by the nozzle. The flow noise sources consist of dynamical and thermodynamic non-uniformities (e.g. turbulence and inhomogeneities, respectively), which are convected downstream in the exhaust jet, and their emission spectrum could make a significant contribution at the frequency of the flow pulsations produced by the turbine rotating at 8 kHz. Turbulent quadrupole noise sources have been extensively studied since the pioneering research of Lighthill (1952, 1954), therefore we shall illustrate the inhomogeneous dipole process of emission, which is associated with the presence of patches of unburned gas, the scale and thence emission frequency of which are determined by the passage through the turbine. These blobs of gas generally have a chemical composition which is distinct from that of the surrounding fluid, and may also be at a different temperature, thus appearing as inhomogeneities in density that are subjected to a displacement force (Campos 1978a) when convected downstream in the mean pressure gradient of the exhaust.

Collections of theoretical data concerning the refraction of sound by jets have been presented by various authors (e.g. Howe 1974). Figure 5 reproduces our own spectra and directivity data, which consist of (i) two spectra in each of eleven directions spaced at intervals of 15° about the vertical ($\theta = 90°$), corresponding to the two sets of scales in (49), and (ii) the total directivities obtained by integrating these spectra along with that for a plane interface (solid line). For our simulation of Concorde at take-off conditions, the lower and upper limits of the frequency band and the decibel level of the spike are given in table 6 [in which the values in brackets correspond to the larger shear-layer scales, the second set of values in (48a, c)]. The direction of undeflected transmission, predicted theoretically from (31), is $\theta_s = 114\cdot6°$, and this corresponds to the absence of attenuation associated with scattering by interfacial irregularities, i.e. the attenuation is due only to diffraction by turbulence. It appears from the spectra that the spike at 105° and 120° is rather higher than that at the vertical ($\theta = 90°$), even though the source is a vertical dipole, showing the significance of the decreased attenuation at or near to the direction of undeflected transmission; the attenuation associated with diffraction by turbulence increases monotonically away from the vertical, thus the spike at 120° is slightly lower than that at 105°. No spike is received at 135° and 150° because the re-radiating element in the line of sight from the observer to the source lies in a grazing direction (i.e. below the mean slope of the interface, which is given by (35b) as $\theta_* = 54\cdot9°$ or $125\cdot1°$) and the energy of the spike
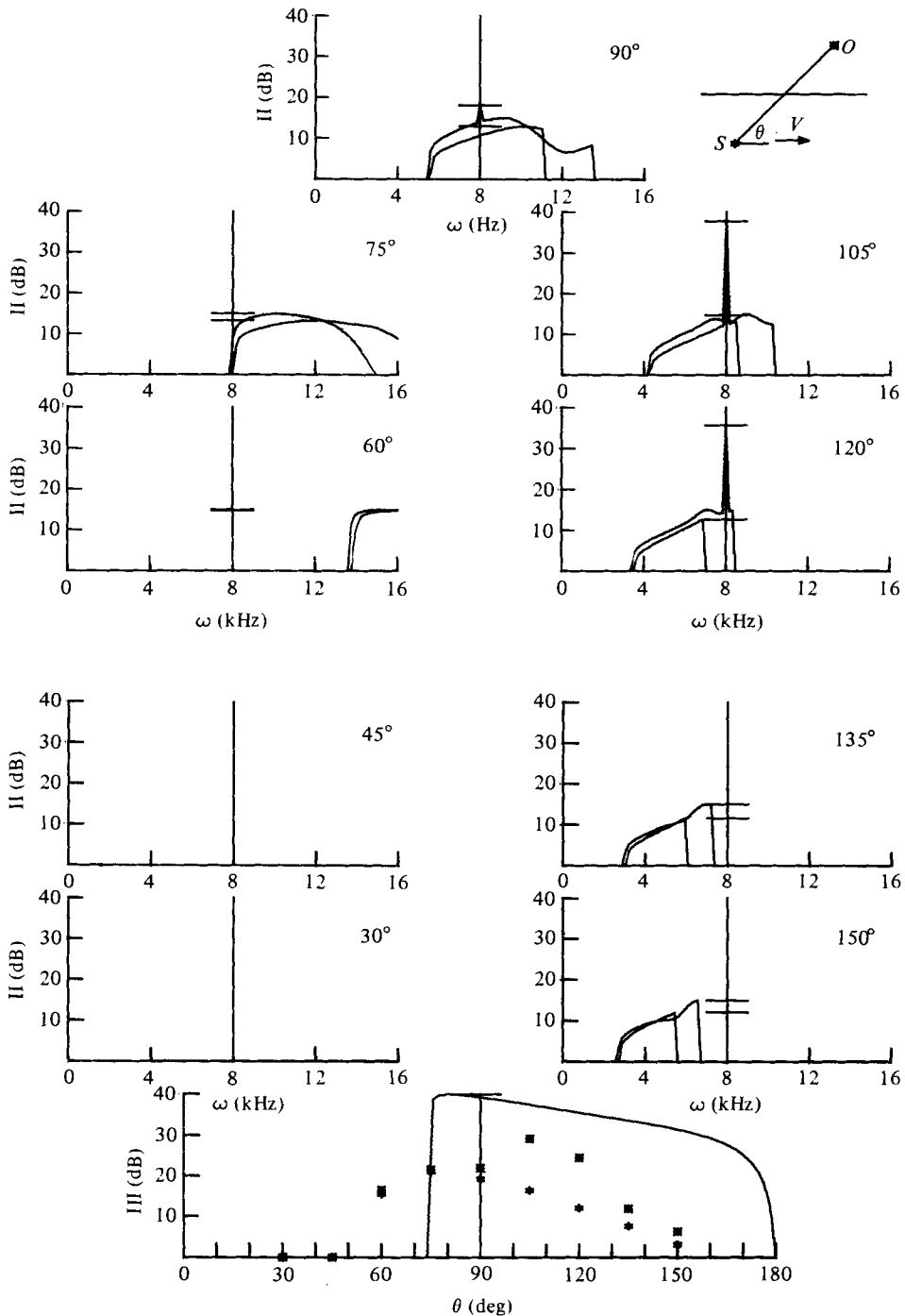
FIGURE 5. Spectra and directivity data for simulation of Concorde noise at take-off. $M = 2 \cdot 000$, $L = 125$ mm, $f = 8$ kHz, $d = 0 \cdot 3000$, $c = 1 \cdot 800$, $b = 50$ mm, $a = 40$ mm, vertical dipole.

Angle θ	Limits of the broad band (kHz)		Peak level (dB)
	Lower	Higher	
30°	– (–)	–	– (–)
45°	– (–)	–	– (–)
60°	13·76 (13·92)	> 16·0 (> 16·0)	15·0 (14·8)
75°	8·00 (8·16)	14·89 (> 16·0)	15·0 (13·3)
90°	5·60 (5·58)	13·44 (11·04)	18·1† (13·0)
105°	4·32 (4·28)	10·24 (8·48)	37·7† (14·8†)
120°	3·52 (3·51)	8·32 (6·88)	35·7† (12·6)
125°	3·04 (3·05)	7·20 (5·92)	15·0 (11·6)
150°	2·72 (2·88)	6·56 (5·44)	15·0 (12·1)

† Spike.

TABLE 6

is re-scattered into other directions (forming a diffuse sound field which we have neglected). The angle of total internal reflexion for a plane interface [given by (33) for the conditions (50)] is $\theta_+ = 74\cdot7°$ and no spike is transmitted into the directions further to the rear; the latter would form the 'zone of silence' of a plane interface, into which the turbulent and irregular shear layer [described by (49)] can effectively radiate a broad band (e.g. at 60°). The bands are biased towards high frequencies in the rear arc ($\theta < 90°$) and, conversely, towards low frequencies in the forward arc ($\theta > 90°$), a property which was predicted generally in § 3.3, noted for the high speed directional spectra in figure 2 (a), and observed experimentally for low speed jets by Candel, Julienne & Julliand (1975). Doubling the effective thickness of the turbulent region and the r.m.s. height of interfacial irregularities does not affect the bands as much as the spike, the latter being totally absorbed into the broad-band radiation in all directions except 105°, where the spike was formerly most prominent and is now barely discernible.

This attenuation effect can be appreciated in the directivity plot in figure 5, or in table 7, which lists (i) the directivity for a plane interface devoid of turbulence, (ii) the directivity for a turbulent and irregular shear layer with the scales indicated first in (49a–c), (iii) the directivity for the shear layer with 'doubled scales' [second values in (49a,c)] and (iv) the attenuation given by (iii) in comparison with that in (ii). The degree of attenuation (iv) is small (< 4 dB) for all directions in which the spectrum is essentially a broad band, and is significant (> 12 dB) where (e.g. at 105° and 120°) a spike has been absorbed. The maximum of the directivity is thus shifted from the forward arc (105°) to the rear arc (75°, where it would be for a plane interface), and the peak level is reduced by 8·0 dB (in addition to the 10·6 dB reduction given by the present shear layer compared with a theoretical smooth layer devoid of turbulence).

These results lead to the following conclusions concerning the application of the phenomenon of spectral broadening to the reduction of the noise disturbance of modern jet-powered aircraft, such as Concorde: (a) if the noise spectrum (for the existing shear layer) consists of only a broad band devoid of spikes, increasing the degree of irregularity and/or the thickness of the shear layer is unlikely to provide a worthwhile degree of attenuation, and might actually have the opposite effect, by

Case Angle θ	(i) Plane (dB)	(ii) Present (dB)	(iii) Doubled (dB)	(iv) Variation ($\pm$ dB)
30°	†	†	†	†
45°	†	†	†	†
60°	†	16·5	15·6	−0·9
75°	39·8‡	21·6	21·2‡	−0·4
90°	39·0	22·0	19·3	−2·7
105°	37·6	29·2‡	16·5	−12·7‡
120°	35·3	24·5	12·1	−12·4
135°	33·6	12·0	7·7	−4·3
150°	31·2	6·4	3·2	−3·2

† $\leqslant$ 0 dB.   ‡ Extrema (i.e. maximum of directivity or minimum variation).

TABLE 7

increasing the extent of the turbulent and inhomogeneous regions which can contribute to noise generation; (b) if the spectrum contains prominent and audibly objectionable spikes, in particular spikes emitted by mechanical sources located within the engine nacelle and/or radiated by flow sources convected in the exhaust jet, then a shear layer which is effectively thicker and more sinuous can smooth the spectrum, transferring energy from the spikes into the bands to result in an overall reduction of the noise level by as much as one audible order of magnitude (10 dB). Specifically, for the shear layer of a turbojet-engine exhaust, which is irregular and contains turbulence with mostly longitudinal orientation (i.e. in planes perpendicular to the nozzle lip), by causing the refraction scale in the direction transverse to the jet velocity to be of magnitude comparable to the longitudinal refraction length L (and also, possibly, a refraction time $L_0 \simeq L/c_0$), the associated increase in scattering and diffraction may provide considerable attenuation. These effects underlie the design of the corrugated exhaust nozzles of the first generation of jet airliners (Lighthill 1962), and a careful optimization of the refraction properties of the shear layer could possibly provide an attenuation comparable to that which is obtained currently by means of additional shear layers (e.g. an auxiliary jet acting as a noise shield, such as the by-pass flow of a turbofan engine). It is emphasized, in connexion with the modelling of experiments, that the statistical parameters (refraction scales, mean height of irregularities and effective thickness of the region of turbulence) of the shear layer can be measured by using a test source in the jet to obtain a calibration spectrum, the theory then predicting (at the same station) the spectra for other source multipoles, emission frequencies and observation angles. In simple terms, transverse (and unsteady) as well as longitudinal convected irregularities and turbulent perturbations can redistribute internal noise over a wider range of directions and also over a broader spectrum of frequencies, with a possibly significant reduction in the noise disturbance caused by current jet-powered aircraft.

I record my appreciation of the work of Candel, Julienne & Julliand (1975) and of Candel, Guédel & Julienne (1975), which provided the experimental evidence of

spectral broadening used in this work. I acknowledge the benefit of many discussions with my supervisor, Dr M. S. Howe, on the means of modelling scattering of sound by shear layers, and also his thorough comments on my drafts. To Professor Sir James Lighthill I owe unfailing and patient encouragement since he gave his attention, in January 1976, to a preliminary version of this work, which has taken long to mature, partly as consequence of other, concurrent tasks (Campos 1977, 1978 a).

REFERENCES

BALSA, T. F. 1976 a The far field of high frequency convected singularities in sheared flows, with an application to jet-noise prediction. *J. Fluid Mech.* **74**, 193–208.

BALSA, T. F. 1976 b Refraction and shielding of sound from a source in a jet. *J. Fluid Mech.* **76**, 443–456.

BARRATT, M. J., DAVIES, P. O. A. L. & FISHER, M. J. 1963 The characteristics of turbulence in the mixing region of a round jet. *J. Fluid Mech.* **16**, 337–367.

BECKMANN, P. & SPIZZICHINO, A. 1963 *The Scattering of Electromagnetic Waves from Rough Surfaces.* Pergamon.

BERRY, M. V. 1973 The statistical properties of echoes diffracted from rough surfaces. *Phil. Trans. Roy. Soc.* A **273**, 611–654.

BORN, M. & WOLF, E. 1970 *Principles of Optics*, 5th edn. Pergamon.

CAMPOS, L. M. B. C. 1977 On the generation and radiation of magneto-acoustic waves. *J. Fluid Mech.* **81**, 529–549.

CAMPOS, L. M. B. C. 1978 a On the emission of sound by an ionized inhomogeneity. *Proc. Roy. Soc.* A **343**, 65–91.

CAMPOS, L. M. B. C. 1978 b The spectral broadening of sound by turbulent shear layers. Part 1. On the transmission of sound through turbulent shear layers. *J. Fluid Mech.* **89**, 723–749.

CANDEL, S. M., GUÉDEL, A. & JULIENNE, A. 1975 Refraction and scattering of sound in an open wind tunnel flow. *Proc. 6th Int. Cong. Instrum. in Aerospace Simulation Facilities, Ottawa*, p. 288.

CANDEL, S. M., JULIENNE, A. & JULLIAND, M. 1975 Étude de l'effet de masque produit par un écran fluide. *Dép. Aérodyn. Acoust., Direction Tech., SNECMA, Villaroche, Paris, Fiche Tech.* YKA 869.

CHERNOV, L. A. 1967 *Wave Propagation in a Random Medium.* Dover.

CLARKE, R. H. 1973 Theory of acoustic propagation in a variable ocean. *Saclant ASW Res. Centre, La Spezia, Memo.* SM-28.

COURANT, R. & HILBERT, D. 1966 *Methods of Mathematical Physics.* Interscience.

FFOWCS WILLIAMS, J. E. 1974 Sound production at the edge of a steady flow. *J. Fluid Mech.* **66**, 791–816.

HAMMERSLEY, J. M. & HANDSCOMB, D. C. 1960 *Monte Carlo Methods.* Methuen.

HERMITE, C. 1864 Sur un nouveau dévelopement en séries de fonctions. *C. R. Acad. Sci. Paris* **53**, 93–100, 266–273.

HOWE, M. S. 1974 Plane wave transmission and reflection coefficients for a two-dimensional jet. *Camb. Univ. Noise Res. Unit. Memo.* MSH/40.

HOWE, M. S. 1975 Application of energy conservation to the solution of radiation problems involving uniformly convected source distributions. *J. Sound Vib.* **43**, 77–86.

HOWE, M. S. 1976 The attenuation of sound by a randomly irregular impedance layer. *Proc. Roy. Soc.* A **347**, 513–535.

JEFFREYS, H. & JEFFREYS, B. S. 1946 *Methods of Mathematical Physics.* Cambridge University Press.

JONES, D. S. 1974 A linear model of a finite amplitude Helmholtz instability. *Proc. Roy. Soc.* A **338**, 17–41.

JONES, D. S. 1977 The scattering of sound by a simple layer. *Phil. Trans. Roy. Soc.* A **284**, 287–328.

LANDAU, L. D. & LIFSHITZ, E. M. 1959 *Fluid Mechanics.* Pergamon.

LIGHTHILL, M. J. 1952 On sound generated aerodynamically. I. The general theory. *Proc. Roy. Soc.* A **211**, 564–587.

LIGHTHILL, M. J. 1954 On sound generated aerodynamically. II. Turbulence as a source of sound. *Proc. Roy. Soc.* A **222**, 1–32.

LIGHTHILL, M. J. 1958 *Fourier Transforms and Generalised Functions.* Cambridge University Press.

LIGHTHILL, M. J. 1962 Sound generated aerodynamically. Bakerian lecture (1961). *Proc. Roy. Soc.* A **252**, 147–182.

MANI, R. 1976 The influence of flow on jet noise. *J. Fluid Mech.* **73**, 773–778, 779–793.

PHILLIPS, O. M. 1960 On the generation of sound by supersonic turbulent shear layers. *J. Fluid Mech.* **9**, 1–28.

RAYLEIGH, LORD 1873 Note on a natural limit to the sharpness of spectral lines. *Nature* **8**, 474–475. (See also *Papers*, vol. 1, pp. 83–84.)

RAYLEIGH, LORD 1889 On the limit to interference when light is emitted from moving molecules. *Phil. Mag.* **27**, 298–304. (See also *Papers*, vol. 3, pp. 258–263.)

RAYLEIGH, LORD 1915 On the widening of spectrum lines. *Phil. Mag.* **29**, 274–284. (See also *Papers*, vol. 6, pp. 291–299.)

RAYLEIGH, LORD 1945 *The Theory of Sound.* Dover.

SHOLNIK, M. I. 1962 *Introduction to Radar Systems.* McGraw-Hill.

WATSON, G. N. 1927 *Theory of Bessel Functions*, 4th edn. Cambridge University Press.